Maintenance of the marginal-zone B cell compartment specifically requires the RNA-binding protein ZFP36L1

Newman, Rebecca; Ahlfors, Helena; Saveliev, Alexander; Galloway, Alison; Hodson, Daniel J; Williams, Robert; Besra, Gurdyal S; Cook, Charlotte N; Cunningham, Adam F; Bell, Sarah E; Turner, Martin

DOI:
10.1038/ni.3724

Document Version
Peer reviewed version

Citation for published version (Harvard):
Newman, R, Ahlfors, H, Saveliev, A, Galloway, A, Hodson, DJ, Williams, R, Besra, GS, Cook, CN, Cunningham, AF, Bell, SE & Turner, M 2017, 'Maintenance of the marginal-zone B cell compartment specifically requires the RNA-binding protein ZFP36L1', *Nature Immunology*, vol. 18, pp. 683–693. https://doi.org/10.1038/ni.3724

The RNA Binding Protein ZFP36L1 Maintains Marginal Zone B cells

Rebecca Newman[1,2], Helena Ahlfors[1], Alexander Saveliev[1], Alison Galloway[1], Daniel J Hodson[3], Robert Williams[1], Charlotte N Cook[4], Adam F Cunningham[4], Sarah E Bell[1], Martin Turner[1]*

AFFILIATIONS

[1]Laboratory of Lymphocyte Signalling and Development, The Babraham Institute, Babraham Research Campus, Cambridge, CB22 3AT, United Kingdom.

[2] Immune Receptor Activation Laboratory, The Francis Crick Institute, 1 Midland Road, London, NW1 1AT, United Kingdom.

[3]Department of Haematology, University of Cambridge, The Clifford Allbutt Building, Cambridge Biomedical Campus, Hills Road, Cambridge, CB2 0AH, United Kingdom.

[4]MRC Centre for Immune Regulation, School of Immunity and Infection, University of Birmingham, Birmingham, B15 2TT, United Kingdom.

CONTACT INFORMATION

martin.turner@babraham.ac.uk

ADDITIONAL TITLE PAGE FOOTNOTES

Role of Zfp36l1 in MZ B cells

Abstract

RNA binding proteins (RBP) of the ZFP36 family are best known for inhibiting the expression of cytokines through binding to AU rich elements in the 3'UTR and promoting mRNA decay. Here we show an indispensible role for ZFP36L1 as the regulator of a post-transcriptional hub that determines the identity of Marginal Zone (MZ) B cells promoting their proper localization and survival. ZFP36L1 controls a gene expression program related to signaling, cell-adhesion and locomotion, in part, by limiting the expression of the transcription factors KLF-2 and IRF-8 that are known to enforce the follicular B cell phenotype. These mechanisms emphasize the importance of integrating transcriptional and post-transcriptional processes by RBP for maintaining cellular identity between closely related cell types.

Introduction

Marginal zone (MZ) B cells surround the B cell follicles of the spleen and are continuously exposed to blood-borne antigens. This positioning of MZ B cells enables them to provide immune surveillance of the circulatory system, and shuttle antigen to FDCs (follicular dendritic cells)[1, 2]. Their localization to the MZ and characteristic migratory potential, to and from the B cell follicle, also contributes to their maintenance through the provision of survival signals [2, 3, 4, 5]. The low activation threshold of MZ B cells enables an immediate antibody response prior to the production of high-affinity antibody. Upon antigen encounter, MZ B cells are poised to promote T cell activation by presenting antigen as well as differentiating into plasmablasts[6]. Compared to follicular (FO) B cells, MZ B cells express greater amounts of surface IgM, CD35, CD21 and CD1d. Together with elevated expression of toll-like receptors (TLR) these features facilitate rapid responses against blood-borne pathogens such as encapsulated bacteria[7, 8].

MZ B cells develop from transitional-2 (T2) B cells via an intermediary population of marginal zone precursor (MZP) B cells which display high cell surface expression of the complement receptors CD35 (CR1) and CD21 (CR2) and IgM, whilst retaining some hallmarks of immaturity, including expression of CD93[9]. Selection into the MZ B cell lineage is dependent upon signaling by membrane immunoglobulin, and by NOTCH2 and the BAFF-R[7 9]. MZ and FO B cells can be separated on the basis of their gene expression profiles[10], and the differences in their transcriptomes contribute to the differential development, localization and function of these cells. Consistent with this, transcriptional regulators have been shown to have specific roles in MZ and FO B cells. Of these, NOTCH2 plays a gene dose-dependent and non-redundant role in promoting the MZ B cell fate[11, 12], and signaling through the NOTCH2 receptor is essential for the retention of B cells in the MZ[4]. Interferon Regulatory Factor (IRF)-4, and the related IRF-8 limit the size of MZ B cell pool[13], and IRF-4 regulates the positioning of cells in the MZ by restricting NOTCH2 function. Krüppel-like factor (KLF)-2 enforces the FO B cell phenotype. In its absence, the MZ B cell pool is expanded and FO B cells show the signaling and migration characteristics of MZ B cells[14, 15]. By contrast, KLF3 promotes the persistence of MZ B cells and may antagonise the activity of KLF2[16]. These factors are frequently mutated in splenic MZ lymphoma[17], suggesting they may also form part of a network that sustains the survival and localization of MZ B cells in pathological situations. Thus the interrelationship between transcriptional regulation, signal transduction and cell positioning for the development and survival of MZ B cells needs to be further understood[17]. Despite this, central regulators of this network have yet to be described.

The post-transcriptional control of RNA is a mechanism of gene regulation that brings about changes in the transcriptome through alterations in RNA processing and stability; it also regulates the proteome through changes in the tempo or location of mRNA translation. These versatile mechanisms, which are directly regulated by RNA binding proteins (RBP), as well as non coding RNAs, complement transcriptional control and add robustness to gene regulatory networks[18]. Profiling of microRNAs indicated that, when compared to FO B cells, MZ B cells contained fewer microRNAs, and deletion of Dicer[19], or microRNA-142[20], led to increased proportions of B cells with a MZ phenotype, suggesting in aggregate that microRNAs suppress MZ formation or survival. Deletion of the well-studied RBPs AUF1[21] or Elavl1 (HuR)[22] in B cells had no effect on MZ numbers. By contrast, retroviral expression of lin28b, acting in haematopoietic stem cells, promoted the development of MZ B cells[23, 24]. Thus the essential post-transcriptional mechanisms governing MZ B cell biology remain to be fully elucidated.

Amongst the more than 1500 RBP in the mammalian genome, the ZFP36 family are characterised by the presence of two highly conserved CCCH-type zinc fingers, which bind RNA. By interacting with Adenosine-uridine-Rich Elements (AREs) in the 3'UTR of mRNAs these RBP promote RNA instability and are an important link between the transcriptome and the proteome[25]. ZFP36 (TTP, Tis11, Nup475, G0S24) has been best characterised as a suppressor of cytokine production in innate immune cells; its relatives ZFP36L1 (Tis11b, BRF1, BERG36, ERF-1) and ZFP36L2 (Tis11d, BRF2, ERF-2) have been shown to play a redundant role during T and B lymphocyte development[26, 27]. The roles of the ZFP36 family during the development and maintenance of mature B-lymphocytes has not been studied. Here we demonstrate the indispensible role of ZFP36L1 in the maintenance of MZ B cells. Through comprehensive analysis of the transcriptomes of primary mouse B cells, and the identification of ZFP36L1 targets in B cells by individual-nucleotide resolution Cross-Linking and Immunoprecipitation (iCLIP), we identify the direct and indirect targets of ZFP36L1 in B cells, and determine a network of factors under the control of ZFP36L1 that sustains MZ B cells. This study demonstrates that cellular identity and ultimately survival is determined by an RNA binding protein.

Results

MZ B cells specifically require ZFP36L1

To identify the roles of the ZFP36 family during lymphocyte development we made use of hCD2-icre, which deletes in early lymphoid progenitors[28], to generate mouse models that are conditionally deficient for *Zfp36* (**Supplementary Fig. 1**), *Zfp36l1* or *Zfp36l2*[26]. MZ B cells were reduced nine-fold following lymphocyte specific deletion of *Zfp36l1* while MZ B cell numbers were normal in mice with a lymphocyte specific deficiency of *Zfp36* or *Zfp36l2* (**Fig. 1a**). In all three models FO B cell numbers were not substantially different from littermate control mice (**Fig. 1b**). Transcripts encoding all three ZFP36 family members are expressed in MZ cells from C57BL/6 mice (**Fig. 1c**), indicating that the specific requirement for ZFP36L1 is not due to cell-specific mRNA expression. Thus, there is a role for ZFP36L1 in the development or maintenance of MZ B cells that cannot be compensated for by ZFP36 or ZFP36L2.

B cell intrinsic requirement for ZFP36L1

Deletion of *Zfp36l1* at the pro-B cell stage, using mb1cre, also led to a loss of MZ B cells (data not shown). To confirm the requirement of ZFP36L1 independently of a role in the bone marrow stages of early B cell development, we generated mice in which *Zfp36l1* is deleted at the T2 B cell stage under the control of CD23cre[29]. In these mice we observed a 10-fold reduction in the number of MZ B cells (**Fig. 2a, b**) and a two-fold reduction in the number of MZP B cells (**Fig. 2d, e**). Peritoneal cavity B cell numbers were also analysed in *Zfp36l1*$^{fl/fl}$mb1$^{cre/+}$ and *Zfp36l1*$^{fl/fl}$ control mice. We observed a small but significant 4-fold decrease in total B1 cells upon *Zfp36l1* deletion with B1a cells and B1b cells equally affected (**Supplementary Fig. 2a-f**). B2 cell numbers in the peritoneal cavity were not different between *Zfp36l1*$^{fl/fl}$mb1$^{cre/+}$ and *Zfp36l1*$^{fl/fl}$ control mice (**Supplementary Fig. a, c**). This small effect on B1 cell numbers contrasts with the much larger effect on MZ B cell numbers

To further understand the role of ZFP36L1 in mature B cells we conditionally expressed a GFP-ZFP36L1 fusion protein[27] using CD23cre. In *Rosa26*^{GFPZFP36L1}CD23$^{cre/+}$ mice GFP-ZFP36L1 expression is evident from the T2 B cell stage (**Supplementary Fig. 2g**). *Rosa26*^{GFPZFP36L1}CD23$^{cre/+}$ mice have a 1.5-fold expanded MZ B cell population, but there are no effects on the numbers of FO B cells and MZP B cells (**Fig. 2f-j**). Examination of MZ B cells by immunofluorescence staining of spleen sections confirms they are much reduced in

number in *Zfp36l1*$^{fl/fl}$CD23$^{cre/+}$ mice and expanded in *Rosa26*^{GFPZFP36L1}CD23$^{cre/+}$ mice (**Fig. 2k, l**). This demonstrates an intrinsic requirement for ZFP36L1 from the T2 B cell stage for the development and/or maintenance of MZ B cells and their precursors.

ZFP36L1 is selectively required for the maintenance of MZ and MZP B cells

To test the continued requirement for ZFP36L1 in B cells we used a cre-oestrogen receptor fusion (ERT2) transgenic in which cre activity is elicited by tamoxifen. As *Zfp36l1* is deleted subsequent to development, a role for this RBP in sustaining MZ B cells can be established. At seven days following tamoxifen treatment, *Zfp36l1*^{flox} was efficiently recombined at the DNA level, and MZ B cell numbers were decreased by 1.3-fold (**Supplementary Fig. 3a-c**). Recombination efficiency of *Zfp36l1* remained high at later time-points, and by day 10 MZ B cells were further decreased by 1.7-fold; and by day 14 a 3.2-fold reduction in number was observed (**Supplementary Fig. 3d-i**). This on-going depletion was selective for MZ B cells as FO B cell numbers were not different at any of the three time-points tested. To exclude that this effect was due to roles of *Zfp36l1* in non-haematopoietic cells[30, 31], we reconstituted irradiated B6.SJL mice with bone marrow from *Zfp36l1*$^{fl/fl}$ERT2$^{cre/+}$ mice, and ERT2$^{cre/+}$ bone marrow as a control group, prior to the administration of tamoxifen (**Fig. 3a**). In this system, *Zfp36l1* deletion is efficient in B cells following tamoxifen treatment (**Fig. 3b**). In the chimeras reconstituted with *Zfp36l1*$^{fl/fl}$ERT2$^{cre/+}$ bone marrow there was a selective loss of MZ and MZP B cells following treatment with tamoxifen (**Fig. 3c, d**), whilst FO and transitional B cell subsets remained unchanged in number compared to the ERT2$^{cre/+}$-only control chimeras (**Fig. 3e**; data not shown). Therefore *Zfp36l1* is dispensable for the maintenance of FO B cells but necessary for the persistence of MZ and MZP B cells.

To address whether the absence of ZFP36L1 affected cell survival we measured the presence of active caspase-3 by flow cytometry in B cells from these chimeras. An increased proportion of *Zfp36l1*-deficient MZ B cells but not FO B cells were positive for active caspase-3 and thus undergoing apoptosis (**Fig. 3f, g**). The same effect was seen in mice that are conditionally deficient for the RBP (**Fig. 3h, i**). By feeding *Zfp36l1*$^{fl/fl}$mb1$^{cre/+}$ mice 2-bromodeoxyuridine (BrdU) in their drinking water we assessed the turnover of MZ B cells measuring the presence of BrdU labelled cells. During B cell development, BrdU is primarily incorporated into highly proliferative pre-B cells in the bone marrow. In *Zfp36l1*$^{fl/fl}$mb1$^{cre/+}$ mice we observe no change in the entry of BrdU-labeled cells into the FO B cell pool but increased labeling of MZ B cells, and a small decrease of BrdU positive T2 and MZP B cells (**Fig. 3j; Supplementary Fig. 4a)**.

This is consistent with the increased turnover of MZ B cells. By contrast, in the mice expressing GFP-ZFP36L1 (*Rosa26*^{GFPZFP36L1}CD23$^{cre/+}$) BrdU incorporation was decreased in MZ B cells and slightly increased in the T2 and MZP B cells compared to the controls (**Fig. 3k; Supplementary Fig. 4b**). Thus MZ B cells turn over more slowly when they express GFP-ZFP36L1. Taken together these data indicate that ZFP36L1 promotes the survival of MZ B cells but is dispensable for the survival of FO B cells.

Gene expression changes following inducible deletion of *Zfp36l1*

As *Zfp36l1* controls gene expression by promoting RNA decay[25, 27], its direct targets will be a subset of those RNAs that show increased expression in mutant cells. To identify these we first performed RNAseq on sorted MZ B cells from tamoxifen treated *Zfp36l1*$^{fl/fl}$ERT2$^{cre/+}$ and ERT2^{cre} mice. The elective deletion of *Zfp36l1* was efficient as we observed a significant decrease in the number of reads mapped within the floxed region of the gene, and most of the remaining reads were found to map to exon 1 that lies outside of the floxed region (**Supplementary Fig. 5a**). Upon loss of *Zfp36l1* we observed significant (padj<0.01) increases in the expression of 330 transcripts and diminished expression of 215 transcripts. Of these, 84 and 26 transcripts were increased or decreased in expression by greater than 1.5 fold respectively (**Fig. 4a; Supplementary table 1**). The 50 transcripts that showed the greatest changes in expression are illustrated as a heatmap in supplementary figure 5. We observed an increase in the expression of Zfp36l2 (**Fig. 4a; Supplementary Fig. 5b**), further indicating that ZFP36L2 cannot compensate for ZFP36L1 in MZ B cells.

The direct targets and the specific nucleotide contacts between ZFP36L1 and RNAs can be identified by iCLIP, but this method has a requirement for large numbers of cells and it is not sensitive enough to apply to MZ B cells. Nevertheless, we attempted to identify ZFP36L1 targets by making use of ZFP36L1 iCLIP data from activated FO B cells[27]. Although the iCLIP has not been performed on MZ B cells it identifies candidate mRNAs that can be bound by ZFP36L1. Thus 73 genes with increased expression, 11 of which were increased by a fold change of greater than 1.5 (**Fig. 4b; Supplementary table 2, 3**), are identified as possible direct targets of ZFP36L1 in MZ B cells. 24 transcripts with diminished expression in MZ B cells were also found to overlap with the iCLIP data, however only a single transcript (*Per2*) exhibited a fold change of greater than 1.5 fold, suggesting that the iCLIP data is a stringent criterion for identifying direct targets of ZFP36L1 in MZ B cells (**Fig. 4b**).

To identify the functional roles of the differentially expressed genes in *Zfp36l1*-deleted MZ B cells we performed a gene set enrichment analysis (GSEA) on all genes that were significantly

altered (padj<0.01) (**Supplementary table 2, 3**). A number of genes found to be differentially expressed were recurrent within distinct GSEA pathways leading to overrepresentation of redundant GO terms. We therefore summarised our GSEA analysis using Revigo to consolidate overlapping GO terms. This way of visualizing the data indicated that there were a substantial number of differentially expressed transcripts involved in signaling; cellular adhesion and migration; the cell cycle and proliferation; and programmed cell death (**Fig. 4c**). Those transcripts that were expressed at reduced amounts did not comprise any common pathway or gene set, which suggests that these genes do not have a common functional role in MZ B cells.

We recently reported evidence of a role for the ZFP36 family of RBP in promoting quiescence[27, 32]. In *Zfp36l1*-deficient MZ B cells, the mRNAs encoding Ccna2, E2f2, Cdc6, Pim1, Ccnd3 and Cdk1 were ≥1.5 fold increased (**Fig. 4c; Supplementary table 1, 2**). To assess whether this had any functional consequences for MZ B cells, we analysed the proportion of MZ B cells expressing the cyclin-dependent kinase inhibitor $p27^{KIP1}$ (*Cdkn1b*) a marker of quiescent cells. The expression of p27 in MZ B cells, and the proportion of p27 positive MZ B cells from tamoxifen-treated *Zfp36l1*$^{fl/fl}$ERT2$^{cre/+}$ mice were unchanged when compared to littermate controls (**Supplementary Fig. 7a-c**), suggesting quiescence was actively maintained. Furthermore, the results of Ki67 and DAPI staining were consistent with this conclusion (**Supplementary Fig. 7d-i**). Thus the reduction of MZ B cells following developmentally programmed or induced deletion of *Zfp36l1* was not due to a loss of quiescence.

ZFP36L1 enforces MZ B cell identity

To further understand the changes in the MZ B cell transcriptome arising from deletion of *Zfp36l1* we compared transcripts that were differentially expressed between *Zfp36l1*-deficient and *Zfp36l1*-sufficient MZ B cells with those that were differentially expressed between wildtype MZ and FO B cells. This revealed that two thirds of the transcripts (54) with the greatest increase in expression in *Zfp36l1*-deficient MZ B cells are normally more highly expressed in FO B cells than in MZ B cells (**Fig. 5a; Supplementary table 4**). This did not reflect contamination of the sorted KO MZ B cells with FO B cells because only a subset of FO B cell enriched transcripts were increased in expression. Some transcripts, which are normally more highly expressed by MZ than FO B cells, (such as PlexinD1 and c-Myc) were also increased in the KO MZ B cells. The differentially expressed transcripts have roles in B cell trafficking, signal transduction and the cell division cycle. Thus in the absence of *Zfp36l1*

the remaining MZ B cells show increased expression of transcripts associated with the FO B cell phenotype.

To determine the effect of GFP-ZFP36L1 on the transcriptome of FO B cells we performed RNAseq and compared the transcriptomes of GFP-ZFP36L1 expressing FO B cells to FO B cells from littermate controls. Pairwise comparison with genes differentially expressed between FO and MZ B cells indicated a trend for GFP-ZFP36L1 positive FO B cells to have increased expression of genes that are preferentially expressed in MZ B cells (**Fig. 5b,** top right hand quadrant**; Supplementary table 5)** and reduced expression of genes characteristically expressed in FO B cells (**Fig. 5b,** bottom right hand quadrant**; Supplementary table 5**). A negative correlation (R=-0.42 of log2FoldChange values) was evident between differentially expressed genes in FO B cells expressing GFP-ZFP36L1 and differentially expressed genes following the loss of ZFP36L1 in MZ B cells (**Fig. 5c**). Transcripts that are increased in *Zfp36l1*-deficient MZ B cells are typically those that are decreased in GFP-ZFP36L1-expressing FO B cells (116 highlighted in red, top left quadrant; **Supplementary table 6**). Moreover, transcripts that are increased in GFP-ZFP36L1-expressing FO B cells are typical of MZ B cells (84 highlighted in red, bottom right quadrant; **Supplementary table 6**). This supports the hypothesis that ZFP36L1 is required to maintain MZ B cell identity.

We next examined cell surface markers expressed by FO B cells from *Rosa26*^{GFPZFP36L1}CD23$^{cre/+}$ mice. GFP-ZFP36L1 expressing FO B cells showed increased expression of CD21, CD1d and MHCII (**Fig. 5d**), indicating that their surface phenotype and "activation" status resembled MZ B cells. Furthermore, immunofluorescence of spleen sections showed increased CD1d^{+} cells, which also express IgD, residing within the follicle of *Rosa26*^{GFPZFP36L1} CD23$^{cre/+}$ mice compared to controls (**Fig. 2k; Supplementary Fig. 8a white arrowheads**). As a number of the differentially expressed transcripts we identified had roles in cell signaling we measured calcium flux elicited by surface IgM crosslinking in *Zfp36l1*-deficient MZ B cells. Enhanced BCR elicited calcium flux is a hallmark of the MZ phenotype compared to FO B cells[33] and we observed this phenomenon in control littermate mice (**Fig. 5e, f**). However, calcium flux was reduced in *Zfp36l1*-deficient MZ B cells to the level of FO B cells (**Fig. 5e**), but was not altered in *Zfp36l1*-deficient transitional B cell subsets (data not shown) or FO B cells (**Fig. 5e**). Pre-treatment with EGTA, to chelate extracellular calcium, reveals the defective release of calcium from the internal stores of *Zfp36l1*-deficient MZ B cells (**Fig. 5f**). Thus one role of ZFP36L1 in MZ B cells is to enhance BCR signaling. Taken together, these data suggest that ZFP36L1 enforces the phenotype of MZ B cells. To test for

functional defects of the residual MZ B cells, we immunized *Zfp36l1*$^{fl/fl}$CD23$^{cre/+}$, *Rosa26*^{GFPZFP36L1} CD23$^{cre/+}$ and littermate control mice with the CD1d-restricted antigen NP-α-GalCer[34]. NP-specific antibody titres from sera taken at day-4 post immunization produced are not different when comparing *Zfp36l1*$^{fl/fl}$CD23$^{cre/+}$ and *Zfp36l1*$^{fl/fl}$ control mice, indicating MZ B cell numbers in the knockout are not limiting in the response of MZ B cells to antigen *in vivo* (**Supplementary Fig. 8b**). There was a small increase in serum NP-IgM in mice expressing the GFP-ZFP36L1 fusion protein, which may reflect increased numbers of MZ B cells in these mice. Overall this data indicates little evidence for a role of ZFP36L1 in the response of MZ B cells to antigen *in vivo*/CD1d restricted humoral responses *in vivo*.

ZFP36L1 targets transcription factors important for MZ B cell identity and survival

IRF8 mRNA was increased 1.3-fold (padj<0.0002) in MZ B cells in the absence of ZFP36L1 (**Fig. 6a**), and was decreased in expression in GFP-ZFP36L1-positive FO B cells (**Fig. 6b**). IRF8 protein expression was also elevated in *ZFP36l1*-deficient MZ B cells (**Fig. 6c, d**). Irf8 mRNA contains a highly conserved ARE in its 3'UTR and was bound by ZFP36L1 in the iCLIP assay (**Fig. 6e**), indicating it is a likely direct target of ZFP36L1 in MZ B cells. A role for IRF8 in limiting MZ B cell numbers is suggested by data showing loss of IRF8 leads to an enlarged MZ B cell compartment[13]. To assess whether IRF8 target genes are likely to contribute to the observed MZ phenotype, we determined if the differentially expressed transcripts in our RNAseq data from *Zfp36l1*-deficient MZ B cells were also identified as IRF8 targets in high quality ChIP-seq data[35]. This indicated that a subset of "FO-signature" genes expressed by *Zfp36l1*-deficient MZ B cells are bound by IRF8 (**Fig. 6f**), suggesting that increased expression of IRF8 contributes directly to the altered expression of these genes in the absence of ZFP36L1. By assessing the distribution of direct ZFP36L1 targets identified by the iCLIP and IRF8 target genes amongst differentially expressed transcripts, we observed minimal overlap of the majority of ZFP36L1 targets (shown in black in **Fig. 6g**) with highly differentially expressed IRF8 targets (shown in dark green, **Fig. 6f**). This indicates that ZFP36L1 and IRF8 generally act in a hierarchical manner whereby ZFP36L1 targets a range of genes including IRF8, which in turn targets genes important for cell survival, localisation, signaling and MZ B cell identity.

KLF2 mRNA was 3.1 fold increased in *Zfp36l1*-deficient MZ B cells (**Fig. 4a; 7a**). KLF2 protein was also increased in *Zfp36l1*-deficient MZ B cells as assessed by flow cytometry (**Fig. 7b, c**). Klf2 mRNA contains a TATTTATT ARE in its 3'UTR, which is conserved amongst mammalian

species that have a *Klf2* ortholog (**Fig. 7d; Supplementary table 2**). The binding of ZFP36L1 to this ARE was indicated in our iCLIP analysis (**Fig. 7d**); however the binding did not reach statistical significance due to low KLF2 mRNA abundance in activated B cells[15, 36]. Thus, ZFP36L1 may directly limit expression of KLF2. Mice with KLF2-deficient B cells have a five-fold increase in the number of MZ B cells, and the FO B cells from these mice express increased amounts of a number of genes that are characteristic of MZ B cells[14, 15] indicating that KLF2 suppresses a gene expression programme which underpins the MZ B cell phenotype.

To understand if elevated KLF2 expression contributed to the altered gene expression profile of *Zfp36l1*-deficient MZ B cells we combined ChIPseq data[37] with a microarray analysis of *Klf2*-deficient B cells[14] to generate a list of candidate KLF2 target genes that are relevant to B cells. Next, this gene list was used to identify candidate KLF2 target genes in our transcriptome analysis from wild-type FO and MZ B cells and *Zfp36l1*-deficient MZ B cells. This approach identified a subset of genes that are bound by KLF2; expressed at elevated levels in *Zfp36l1*-deficient MZ B cells; and normally more highly expressed in FO B cells than in MZ B cells (shown in dark blue) (**Fig. 7e**). Furthermore, this analysis showed that among the transcripts increased in *Zfp36l1*-deficient MZ B cells the KLF2-regulated genes are generally absent from both the ZFP36L1 iCLIP dataset and the IRF8 ChIPseq dataset (**Fig. 7f**). This indicates that the observed KLF2 overexpression is consequential for the transcriptome of *Zfp36l1*-deficient MZ B cells and that KLF2 contributes directly to the manifestation of a "FO-signature" transcriptome in *Zfp36l1*-deficient MZ B cells. Taken together, these analyses suggest a model whereby ZFP36L1 limits the expression of a number of genes including the transcription factors IRF8 and KLF2, which in turn regulate genes important for MZ B cell identity and survival (**Supplementary Fig. 8c)**.

ZFP36L1 deficiency results in aberrant trafficking and distribution of B cells

By performing GSEA on 116 transcripts that were both increased in expression in MZ B cells following deletion of *Zfp36l1* and decreased in expression in FO B cells expressing GFP-ZFP36L1 (**Supplementary Fig. 9a**) we identified pathways involved in B cell trafficking; highlighted in red in **Supplementary Fig. 9b**. Flow cytometry analysis demonstrated that there was increased expression of CD62L and β_7 integrin on the cell surface of *Zfp36l1*-deficient MZ B cells and decreased expression of these on GFP-ZFP36L1 positive FO B cells (**Fig. 8a**). We observed little, if any, difference in the expression of CXCR4, CXCR5, β_1 integrin

and LFA-1 (data not shown). Consistent with our RNAseq results (**Supplementary Fig. 9c**), we saw no difference in the expression of CD69 (a surrogate marker for S1Pr1 expression) (**Fig. 8a**). To assess whether the localisation of MZ B cells was altered in the absence of ZFP36L1, we tested the ability MZ B cells to capture CD19-PE from the blood in *Zfp36l1*$^{fl/fl}$CD23$^{cre/+}$ mice. This showed a decreased proportion of CD19-PE positive MZ B cells in the absence of ZFP36L1, suggesting an abnormal localization and/or trafficking of *Zfp36l1*-deficient MZ B cells *in vivo* (**Fig. 8b**).

Immunofluorescence analysis of spleen sections from μMT chimeras with tamoxifen-deleted *Zfp36l1* indicated that an increased proportion of CD1d^{+} MZ B cells were localized in the splenic follicles (**Fig. 8c**). Importantly, these CD1d^{+} cells do not co-express IgD (**Supplementary Fig. 8a white arrowheads**). Quantification of CD1d expression within the splenic follicles (defined by MOMA-1 staining, see **Supplementary Fig. 9e**) demonstrated an increase in the MFI when *Zfp36l1* has been acutely deleted, compared to ERT2$^{cre/+}$ controls (**Fig. 8d**). To confirm that this did not result from increased CD1d expression across all cell types we quantified the MFI of CD1d^{+} cells residing in the MZ (**Supplementary Fig. 9e**). This showed that CD1d expression was comparable between *Zfp36l1*$^{fl/fl}$ERT2$^{cre/+}$ and ERT2$^{cre/+}$ MZ B cells localised within the splenic MZ (**Fig. 8e**). By normalising CD1d MFI within the splenic follicle to overall CD1d expression in the FO and MZ, we confirmed an increased proportion of CD1d^{+} MZ reside in the follicles of *Zfp36l1*-deficient mice (**Fig. 8f**). Thus, ZFP36L1 plays a role in the correct localization of MZ B cells.

Discussion

Here we report the essential role for ZFP36L1 in the maintenance of MZ B cells. The RBP mediates this role by interacting with, and limiting the expression of, a set of transcripts that promote the FO B cell phenotype. The relevant targets of ZFP36L1 in this context are distinct from previously identified targets such as cytokines and drivers of cell cycle progression. This observation is reminiscent of the role of transcription factors which, at discrete stages of B cell development, control the expression of different transcripts characteristic of that developmental stage[38]. It further suggests that ZFP36L1 has the potential to regulate post-transcriptional RNA operons or "regulons"[39] tailored to a specific developmental stage. Consistent with this, ZFP36L1 has been shown to regulate the transcription factor nanog and contribute to differentiation in mouse embryonic stem cells[40]. It can thus be anticipated that ZFP36L1 or its close relatives may play roles in maintaining the distinct identity of other closely related cell types in the immune system; a property previously thought to be exclusive to transcription factors. Such a notion has precedence in other developmental biology systems. In *Caenorhabdtis elegans* the germline and somatic cell fates are regulated by multiple RBPs, many of which contain the tandem CCCH zinc fingers that are characteristic of the ZFP36 family. Amongst these, Oocyte MAturation defective-1[41] and POsterior Segregation-1[42] have been shown to bind with high affinity to AU-rich sequences in 3'UTRs of target mRNAs. Systems analysis indicates extensive crosstalk between RNA binding proteins and transcription factors in *C. elegans*[43]. Our findings may reflect the existence of similar networks in mature B lymphocytes. Thus the ability of RBPs to play a dominant role in directing or maintaining cell fates amongst additional immune cell populations by acting on 3'UTRs deserves further investigation. Formally establishing this mechanism in lymphocytes will require both the identification of the relevant RBP, as we have done here, and demonstrating the necessity for sequences in 3'UTRs bound by the RBP for the maintenance of cellular identity.

As the RNA binding domains of each ZFP36 member are highly related in sequence, and redundancy between co-expressed family members is frequently found, the unique role for *Zfp36l1* that we have found here in MZ B cells, which express all three ZFP36 family members, was unanticipated. The specific requirement for *Zfp36l1* in B cells for the MZ B cell compartment may reflect differences in the post-translational biology of the encoded RBPs, such as the effects of specific phosphorylation or of multi-protein complex formation. Alternatively there may be differences between ZFP36 family members in their ability to bind to and regulate specific targets. Our data indicate that the mRNA encoding the related

ZFP36L2, which acts redundantly with ZFP36L1 in the thymus and bone marrow, was bound by ZFP36L1, and the abundance of ZFP36L2 was substantially increased in ZFP36L1-null MZ B cells. However, unlike the situation in early lymphocyte development, ZFP36L2 could not compensate for the absence of ZFP36L1 in MZ B cells. Extensive further work is required to understand the molecular basis for the redundant and non-redundant functions of these RBPs.

While the role of *Zfp36l1* in the maintenance of MZ B cells is mediated by the repressive effects of this RBP on the B cell transcriptome there are a number of indirect changes in the transcriptome that follow from the enhanced expression of ZFP36L1 targets. This suggests that the transcriptome of MZ B cells is determined by network of factors, acting transcriptionally and post-transcriptionally, in which ZFP36L1 is a major hub (**Supplementary Fig. 8b**). Here we have focussed on two direct targets of ZFP36L1, identified by our iCLIP analysis, IRF8 and KLF2, which in turn regulate a number of downstream genes important for MZ B cell identity. Many, but not all, of the indirect changes in the transcriptome of *Zfp36l1* deficient MZ B cells appeared to stem from the increased expression of IRF8 or KLF2 (these transcription factors account for 18/54 differentially expressed "FO signature" genes). Many KLF2 targets, that were not ZFP36L1 targets, were increased following loss of *Zfp36l1* and a number of these were also suppressed in the GFP-ZFP36L1 expressing FO B cells. Overall the phenotype of *Zfp36l1*-deficiency in mature B cell development has similarities to that of B cells with mutated KLF3, a transcription factor that appears to act as a transcriptional repressor of KLF2[16]. Conversely, transgenic B cells overexpressing KLF3 have a similar phenotype to GFP-ZFP36L1 expressing B cells[44]. The molecular basis for KLF2 and KLF3 regulation of trafficking in B cells remains relatively poorly understood, as it appears to affect responses to chemokines in both MZ and FO B cells as well as regulating surface expression of adhesion receptors[45]. IRF8, like IRF4[4], has a role in limiting the size of the MZ B cell pool[13]. Additional ZFP36L1 targets amongst the transcripts with increased expression need to be further characterised for their mechanistic roles in peripheral B cell maturation and maintenance, however there is evidence to link many of these to adhesion and metastasis. The kinase Pim1 has been implicated in loss of adhesion and altered cell migration[46, 47]; the transcription factor **Bhlhe40** which has not been functionally characterised at all in B cells but is known to play a role in T cells where it is important for the effects of pertussis toxin[48] and in other cell types Bhlhe40 has been implicated in adhesion and metastasis[49]. Likewise **KIAA0101** (2810417H13Rik) has been associated with metastasis[50]. Much less is known about **Myadm** (myeloid-associated differentiation marker) but it too has been implicated in adhesion[51, 52]. **Txnrd1** (thioredoxin reductase 1) has also been implicated in adhesion and migration[53, 54]. We thus suggest that ZFP36L1 serves to coordinate the abundance of proteins that act at

many different stages in the cell biology of adhesion and migration. These examples form the basis of a network of transcriptional and post-transcriptional interactions that "lock-in" cell specific transcriptomes. There is an enhanced regulatory flexibility conferred by dual transcriptional and post-transcriptional control, as pathways that are under the control of different transcription factors may be strongly coordinated by RNA binding proteins.

The small decrease in the number of MZP B cells in the spleen when B cells specifically lack ZFP36L1, contrasts with the phenotype of mice in which NOTCH2 signalling is attenuated [11, 12, 55] and suggests that ZFP36L1 plays a minimal role in the development of MZ B cells but is primarily required for the persistence of MZ B cells *in vivo*. The FO B cell pool and its precursor populations are intact in the absence of ZFP36L1 indicating that this RBP plays no obvious role in FO B cell development and/or maintenance. As we did not observe an apoptosis gene expression signature in our RNAseq analysis that was regulated directly by ZFP36L1 it is likely that this apoptosis arises indirectly due to a loss of cellular identity and abnormal adhesion and migration. The maintenance of the MZ phenotype and survival may be affected by the intrinsic signaling capability of membrane immunoglobulin, which was reduced in MZ B cells lacking ZFP36L1, and has also been linked previously to the adhesive and motile capacity of MZ B cells. Some of these mechanisms are finely balanced as evidenced by their sensitivity to gene dosage. Instead, the interaction between MZ B cells and unique extracellular matrix components that are enriched in the MZ, and play an important role in promoting the survival of MZ B cells[3], may be perturbed. These mechanisms protect MZ B cells from apoptosis. It is therefore tempting to speculate that *Zfp36l1*-deficient MZ B cells are lacking these pro-survival signals when access to the MZ is limited. This may be analogous to the process of anoikis whereby detachment of adherent cells from a niche can lead to programmed cell death[56].

In summary, our data suggest that ZFP36L1 acts post-transcriptionally to enforce the phenotype of MZ B cells and in its absence MZ B cells are mislocalized and die. It will be important for future studies to establish whether these mechanisms contribute to pathology in lymphoma or autoimmune disease.

Acknowledgments

We thank Meinrad Busslinger, Michael Reth, Thomas Ludwig and Dimitris Kioussis for cre-expressing mice. This work was funded by a GSK-CASE studentship to RN and funding from the Biotechnology and Biological Sciences Research Council, The Medical Research Council and Bloodwise. We thank Kirsty Bates, Rachael Walker, Arthur Davies and Lynzi Waugh and members of the Biological Services Unit for technical support; Donald Bell and Pavel Tolar for help with immunofluorescence analysis; members of the laboratory, Louise Webb, Michelle Linterman and Tal Arnon for helpful advice.

FIGURE LEGENDS

Figure 1: MZ B cells specifically require ZFP36L1

Number of (**a**) MZ B cells (**b**) FO B cells from the spleens of ZFP36 family conditional knockout mice assessed by flow cytometry. Each symbol represents data from an individual mouse. Data were analysed using a Mann-Whitney test. (**c**) ZFP36 family relative mRNA expression in sorted MZ B cells. Bars are representative of 3 biological replicates, error bars represent SEM.

Figure 2: B cell intrinsic requirement for ZFP36L1

Flow cytometric analysis of splenic B cells from *Zfp36l1*$^{fl/fl}$CD23$^{cre/+}$ and *Rosa26*^{GFPZFP36L1}CD23$^{cre/+}$ mice. Dot plots are pre-gated on (**a, f**) B220^{+}CD93^{-} cells (**e, j**) B220^{+}CD93^{+} cells. Numbers indicate the percentage of cells within the gate. Data are representative of at least 6 mice per genotype. Absolute number of (**b, g**) MZ B cells (**c, h**) FO B cells (**d, i**) MZP assessed by flow cytometry. Data on all graphs were analysed using a Mann-Whitney test. (**k**) Immunofluorescence analysis of spleen sections from *Zfp36l1*$^{fl/fl}$CD23$^{cre/+}$ mice, *Rosa26*^{GFPZFP36L1}CD23$^{cre/+}$ mice and a *Zfp36l1*$^{fl/fl}$ control. Sections were stained with either anti-CD1d (magenta), anti-IgD (cyan) and anti-CD169 (green) or anti-IgM (magenta) and anti-CD169 (green). All images were captured at 10x magnification, scale bars are shown. (**l**) Quantification of CD1d^{+} MZ width. Multiple measurements were taken using Image-J (NIH) from at least 10 separate follicles per genotype. Data were analysed with Mann-Whitney tests.

Figure 3: ZFP36L1 is selectively required for the maintenance of MZ and MZP B cells

(**a**) Time course depicting generation and analysis of *Zfp36l1*$^{fl/fl}$ERT2$^{cre/+}$ radiation chimeras. (**b**) Relative *Zfp36l1* exon 2 abundance in purified B cells assessed by qPCR in tamoxifen treated chimeras. Data are representative of two independent experiments (n=6 mice per group in each experiment). Numbers of (**c**) MZ B cells (**d**) MZP (**e**) FO assessed by flow cytometry in tamoxifen treated irradiation chimeras. Data are representative of two independent experiments. Data were analysed with a Mann-Whitney test. Proportions of (**f**) MZ B cells (**g**) FO B cells from tamoxifen treated *Zfp36l1*$^{fl/fl}$ERT2$^{cre/+}$ radiation chimeras (open circles) and ERT2$^{cre/+}$ control chimeras (closed circles) staining positive for active caspase3. Data were pooled from two independent experiments. Proportions of (**h**) MZ B cells and (**i**)

FO B cells from *Zfp36l1*$^{fl/fl}$mb1$^{cre/+}$ (open circles) and *Zfp36l1*$^{fl/fl}$ control mice (closed circles) staining positive for active Caspase3. Data were pooled from two independent experiments. Day 14 BrdU incorporation into MZ B cells in (**j**) *Zfp36l*$^{fl/fl}$mb1$^{cre/+}$ conditional knockout mice (open circles) and *Zfp36l1*$^{fl/fl}$ littermate control mice (closed circles) and (**k**) *Rosa26*^{GFPZFP36L1}CD23$^{cre/+}$ (open circles) and *Rosa26*^{GFPZFP36L1} littermate control mice (closed circles). All statistical analysis was performed with a Mann-Whitney test.

Figure 4: Gene expression analysis following deletion of *Zfp36l1*

(**a**) MA plot showing differentially expressed transcripts in red. Cut-off (grey dashed line) is 1.5 fold, padj<0.01. (**b**) Bar chart showing the number of differentially expressed transcripts (padj<0.01), which are increased or decreased in expression, indicating the number of transcripts that overlap with the iCLIP dataset (FDR<0.05) in blue. (**c**) GSEA was carried out using Toppfun tool which is part of ToppGeneSuite for all differentially expressed transcripts (padj<0.01), and summarised using Revigo[57] to remove redundant GO terms. The remaining terms are visualised as a semantic similarity-based scatter plot. Each bubble represents a biological process, size of the bubble represents log(number of genes in each process), and colour is indicative of uniqueness, where red (1) indicates exact overlap with other terms found in the GSEA, and blue (0.6) indicates minimal overlap with other terms found in the analysis.

Figure 5: ZFP36L1 enforces MZ B cell identity

(**a**) Correlation dot plot indicating the differentially expressed transcripts in red (padj<0.01) when comparing *Zfp36l1*$^{fl/fl}$ERT2$^{cre/+}$ (KO) MZ B cells and ERT2$^{cre/+}$ control (WT) MZ B cells to wildtype FO B cell gene expression. Numbers on the plot represent the number of differentially expressed transcripts in each quadrant. Zfp36l1 has been removed from this analysis. (**b**) Correlation dot plot indicating the differentially expressed transcripts in red (padj<0.01) when comparing *Rosa26*^{GFPZFP36L1}CD23$^{cre/+}$ (GFP) FO B cells and *Rosa26*^{GFPZFP36L1} control FO B cells to wild-type MZ B cell gene expression. Numbers on the plot represent the number of differentially expressed transcripts in each quadrant. (**c**) Correlation dot plot showing the relationship between the differentially expressed (padj<0.05) genes (red) found in RNAseq analysis comparing MZ B cells from *Zfp36l1*$^{fl/fl}$ERT2$^{cre/+}$ to ERT2$^{cre/+}$ controls and RNAseq analysis comparing GFP-ZFP36L1 positive FO B cells to FO B cells from littermate controls. Numbers on the plot represent the number of differentially expressed transcripts in each quadrant. (**d**) Expression of “MZ-like” surface markers on FO and MZ B cells from

Rosa26^{GFPZFP36L1}CD23$^{cre/+}$ mice and *Rosa26*^{GFPZFP36L1} littermate controls. (**e**) Calcium flux in MZ B cells and FO B cells following stimulation with anti-IgM. (**f**) Anti-IgM induced calcium flux in MZ and FO B cells following pre-treatment with 10mM EGTA. Black lines indicate *Zfp36l1*$^{fl/fl}$mb1$^{cre/+}$ B cells; grey lines indicate *Zfp36l1*$^{fl/fl}$ B cells from littermate control mice. Data are representative of 3 independent experiments (n=3).

Figure 6: ZFP36L1 regulates IRF8 expression

Normalised read counts for Irf8 in (**a**) MZ B cells from tamoxifen treated mice, which are ERT2$^{cre/+}$ or *Zfp36l1*$^{fl/fl}$ERT2$^{cre/+}$, and (**b**) FO B cells which are *Rosa26*^{GFPZFP36L1} or *Rosa26*^{GFPZFP36L1}CD23$^{cre/+}$. Error bars represent SEM (n=4). (**c**) IRF8 protein expression in MZ B cells from *Zfp36l1*$^{fl/fl}$mb1$^{cre/+}$ conditional knockout mice (black line) and *Zfp36l1*$^{fl/fl}$ control mice (grey filled histogram). A representative of at least 7 mice is shown. (**d**) Summarised FACS analysis showing IRF8 protein expression in MZ B cells from *Zfp36l1*$^{fl/fl}$mb1$^{cre/+}$ conditional knockout mice and *Zfp36l1*$^{fl/fl}$ control mice. Data is pooled from two separate experiments, and analysed using a Mann-Whitney test. (**e**) Conservation of TATTTATTTTT sequence in the 3'UTR of *Irf8* (yellow box) in eutherian mammals. Asterisks denote 100% conservation between all species analysed. Sequences were aligned using ClustalW in Ensembl Perl API. Single nucleotide resolution binding of ZFP36L1 denoted by iCLIP analysis is shown as a blue box. (**f**) Correlation dot plot as in (**Fig. 5a**), showing IRF8 targets in green, which are differentially expressed in our data (dark green) or are not differentially expressed in our data (pale green). (**g**) Correlation dot plot as in **f**, showing iCLIP targets in black, which are differentially expressed in our data (black) or are not differentially expressed in our data (dark grey).

Figure 7: ZFP36L1 regulates KLF2

(**a**) Normalised read counts for Klf2 in MZ B cells from tamoxifen treated mice, which are ERT2$^{cre/+}$ or *Zfp36l1*$^{fl/fl}$ERT2$^{cre/+}$. Error bars represent SEM (n=4). (**b**) KLF2 protein expression in MZ B cells from *Zfp36l1*$^{fl/fl}$mb1$^{cre/+}$ conditional knockout chimeras (black line) and *Zfp36l1*$^{fl/fl}$ control chimeras (grey filled histogram). A representative of at least seven mice is shown. (**c**) Summarised FACS analysis showing KLF2 protein expression in MZ B cells from tamoxifen treated ERT2$^{cre/+}$ and *Zfp36l1*$^{fl/fl}$ERT2$^{cre/+}$ mice. Data were analysed using a Mann-Whitney test. (**d**) Conservation of TATTTATT sequence in the 3'UTR of *Klf2* (yellow box) in mammals which express KLF2. Asterisks denote 100% conservation between all species analysed.

Sequences were aligned using ClustalW in Ensembl Perl API. Single nucleotide resolution binding of ZFP36L1 indicated by iCLIP analysis is shown as a blue box. (**e**) Correlation dot plot as in (**Fig. 5a**), showing B cell specific KLF2 targets in blue, which are differentially expressed in our RNAseq data (dark blue), or are not differentially expressed in our RNAseq data (pale blue). (**f**) Zoomed in correlation dot plot as in (**Fig. 5a**), showing B cell specific KLF2 targets in blue, IRF8 targets in green, ZFP36L1 direct targets identified by iCLIP analysis in cyan, and co-regulated targets (any gene that is identified in at least two datasets) in burgundy.

Figure 8: ZFP36L1 controls MZ B cell localization in the splenic MZ

(**a**) Expression of trafficking molecules in *Zfp36l1* cKO and wildtype MZ B cells, and GFP-ZFP36L1 positive and negative FO B cells. A summary of five mice per genotype is shown. (**b**) Capture of PE-conjugated CD19 by MZ B cells in tamoxifen treated *Zfp36l1*$^{fl/fl}$ERT2$^{cre/+}$ mice and ERT2$^{fl/fl}$ controls. Data were analysed using a Mann-Whitney test. (**c**) Immunofluorescence analysis of splenic sections from tamoxifen treated *Zfp36l1*$^{fl/fl}$ERT2$^{cre/+}$ mice and ERT2$^{fl/fl}$ μMT chimeras. Sections were stained with anti-CD1d (magenta), anti-IgD (cyan) and anti-CD169 (green). All images were captured at 20x magnification, error bars shown. CD1d MFI (-background) was calculated using Image-J (NIH) (**d**) within follicles (defined by MOMA-1 staining, see **Supplementary Fig. 8e**), (**e**) within MZ area (defined by CD1d staining outside of MOMA-1 and IgD staining, see **Supplementary Fig. 8e**), (**f**) Normalised MFI from within follicles/(MFI MZ + MFI FO).

Supplementary Figure 1: Targeting strategy for the generation of *Zfp36*$^{fl/fl}$ mice

(a) The *Zfp36* gene consists of two exons (grey boxes). The targeting vector was designed to introduce loxP sites flanking exon 2, which contains the tandem zinc finger RNA binding domain, and a Neomycin selection cassette (neo) flanked by two FRT sites. The targeting construct was introduced into the *Zfp36* locus of BRUCE4 embryonic stem cells (C57BL/6 origin) by homologous recombination. Positive clones were identified via Southern blotting confirming correct targeting at both 5' and 3' ends. Subsequent crossing of mice possessing the targeted allele to FlpE mice, removing the neo cassette generated the desired *Zfp36*$^{fl/fl}$ mice. The same gene targeting strategy was used to produce *Zfp36l1*$^{fl/fl}$ and *Zfp36l2*$^{fl/fl}$ mice (**b**) Introduction of the hCD2-iCre transgene into homozygous *Zfp36*$^{fl/fl}$ mice caused a tissue specific deletion of exon 2, which was confirmed by Southern blotting.

Supplementary figure 2: Peritoneal cavity B1 require ZFP36L1 and GFP-ZFP36L1 fusion protein is expressed from the transitional 2 B cell stage in *Rosa26*^{GFPZFP36L1}CD23$^{cre/+}$mice

Flow cytometric analysis of peritoneal cavity B cells from *Zfp36l1*$^{fl/fl}$mb1$^{cre/+}$ and *Zfp36l1*$^{fl/fl}$ mice. Dot plots are pre-gated (**d**) B220^{int}CD19^{hi} cells. Numbers indicate the percentage of cells within the gate. Data are representative of at least 8 mice per genotype. Absolute number of (**b**) total B1 cells (**c**) B2 cells (**e**) B1a cells (**f**) B1b cells assessed by flow cytometry. Data on all graphs were analysed using a Mann-Whitney test. (**g**) Flow cytometric analysis of GFP-ZFP36L1 fusion protein expression in splenic B cell subsets from *Rosa26*^{GFPZFP36L1}CD23$^{cre/+}$mice. Black lines are representative of GFP-ZFP36L1 expression in *Rosa26*^{GFPZFP36L1}CD23$^{cre/+}$ mice; grey filled histograms are representative of cre-negative littermate control mice.

Supplementary figure 3: MZ B cells require ZFP36L1 to persist over time

(**a, d, g**) Relative *Zfp36l1* exon 2 abundance in purified B cells assessed by qPCR in tamoxifen treated *Zfp36l1*$^{fl/fl}$ERT2$^{cre/+}$ and ERT2$^{cre/+}$ mice. Absolute numbers of (**b, e, h**) MZ B cells (**c, f, i**) FO B cells assessed by flow cytometry in tamoxifen treated mice. Data were analysed with a Mann-Whitney test. Panels **a**, **b** and **c** show analysis on day 7 following start of tamoxifen treatment, **d, e and f** show day 10 and **g, h and i** show day 14.

Supplementary figure 4: ZFP36L1 controls turnover of MZ B cells

(**a**) Day 14 BrdU incorporation into splenic B cell subsets in *Zfp36l*$^{fl/fl}$mb1$^{cre/+}$ conditional knockout mice (open circles) and *Zfp36l1*$^{fl/fl}$ littermate control mice (closed circles) (**b**) Day 14 BrdU incorporation into splenic B cell subsets from *Rosa26*^{GFPZFP36L1}CD23$^{cre/+}$ and *Rosa26*^{GFPZFP36L1} littermate control mice.

Supplementary figure 5: RNAseq analysis validation

(**a**) Reads mapping to *Zfp36l1*. Reads were mapped using TopHat, and are displayed using IGV. Enrichment of uniquely aligning deduplicated reads shown in grey. The top 4 rows show reads in control (ERT2$^{cre/+}$) replicates, and the bottom 4 rows show reads in KO (*Zfp36l1*$^{fl/fl}$ERT2$^{cre/+}$) replicates. (**b**) Normalised read counts for Zfp36 and Zfp36l2 in MZ B

cells from tamoxifen treated mice which are ERT2$^{cre/+}$ (black bars) or *Zfp36l1*$^{fl/fl}$ERT2$^{cre/+}$ (white bars). Error bars represent SEM (n=4).

Supplementary figure 6: Heatmap illustrating the top 50 regulated genes in *Zfp36l1*$^{fl/fl}$ERT2$^{cre/+}$ MZ B cells compared to ERT2$^{cre/+}$ controls

A clustered heatmap showing the log2 transformed RPKM values of 50 most regulated genes based on their log2FoldChange in the comparison of Zfp36l1$^{fl/fl}$ERT2$^{cre/+}$ MZ B cells to their ERT2$^{cre/+}$ controls. Blue color indicates low, yellow medium and red high expressed genes. Dendrogram shows clustering of the genotypes.

Supplementary figure 7: Normal p27 and Ki67 expression and DAPI profiles in *Zfp36l1*-deficient MZ B cells

(**a**) p27 staining in MZ B cells from *Zfp36l1*$^{fl/fl}$mb1$^{cre/+}$ mice (black line) and *Zfp36l1*$^{fl/fl}$ littermate controls (grey filled histogram) (left panel) and tamoxifen treated *Zfp36l1*$^{fl/fl}$ERT2$^{cre/+}$ (black line) and ERT2$^{cre/+}$ control chimeras (grey filled histogram) (right panel). Isotype control sample (grey line) is shown for both sets of analysis. Summarised analysis showing the proportion of p27^{+} MZ B cells in (**b**) *Zfp36l1*$^{fl/fl}$ and *Zfp36l1*$^{fl/fl}$mb1$^{cre/+}$ mice, (**c**) ERT2$^{cre/+}$ and *Zfp36l1*$^{fl/fl}$ERT2$^{cre/+}$ chimeric mice. Data were analysed using a Mann-Whitney test. (**d**) Ki67 staining in MZ, FO and GC B cells from *Zfp36l1*$^{fl/fl}$mb1$^{cre/+}$ mice (black line) and *Zfp36l1*$^{fl/fl}$ littermate controls (grey filled histogram). FMO control sample (grey line) is shown for all sets of analysis. (**e**) Summarised analysis showing the proportion of Ki67^{+} cells in *Zfp36l1*$^{fl/fl}$mb1$^{cre/+}$ mice (filled circles) and *Zfp36l1*$^{fl/fl}$ mice (open circles). Data were analysed using a Mann-Whitney test. (**g**) DAPI staining in MZ and FO B cells from *Zfp36l1*$^{fl/fl}$mb1$^{cre/+}$ mice and *Zfp36l1*$^{fl/fl}$ littermate controls. Numbers on the graph indicate the percentage of cells in the gate. Summarised analysis showing the proportion of cells in the S/G2-M phase of the cell cycle in (**h**) MZ and (**i**) FO B cells. Data were analysed using a Mann-Whitney test.

Supplementary figure 8: ZFP36L1 regulates localisation, identity and survival

(**a**) Immunofluorescence analysis of spleen sections from *Zfp36l1*$^{fl/fl}$CD23$^{cre/+}$ mice, *Rosa26*^{GFPZFP36L1}CD23$^{cre/+}$ mice. Sections were stained with anti-CD1d (red) and anti-IgD (green). Images were captured at 20x magnification, scale bars are shown. Arrows on the plots indicate colocalization of the stains, or single stained cells only. (**b**) Day 4 NP-specific

IgM endpoint titres from mice immunized with NP-α-GalCer. Data were analysed using a Mann-Whitney test. (**c**) Schematic model depicting the mechanism by which ZFP36L1 regulates survival, migration and identity of MZ B cells through a network of transcription factors which include KLF2 and IRF8.

Supplementary figure 9: ZFP36L1 controls genes involved in mature B cell trafficking

(**a**) Venn diagram indicating the number of overlapping genes, which are increased in *Zfp36l1*-deficient MZ B cells, and decreased in GFP-ZFP36L1 expressing FO B cells using a padj<0.05 cutoff. (**b**) Pathway analysis of genes which are increased in expression in *Zfp36l1* cKO MZ B cells and decreased in expression in GFP-ZFP36L1 expressing FO B cells using a padj<0.05 cutoff. S1pr1 mRNA expression in (**c**) *Zfp36l1*$^{fl/fl}$ERT2$^{cre/+}$ MZ B cells and ERT2$^{cre/+}$ control MZ B cells, and (**d**) *Rosa26*^{GFPZFP36L1}CD23$^{cre/+}$ and *Rosa26*^{GFPZFP36L1} FO B cells. (**e**) Follicular area was defined using MOMA-1 (CD169) staining (green). Follicular area is shown by yellow line. MFI was then calculated for this area. MZ area was defined as CD1d^{+} (magenta) area outside MOMA-1 (green) and IgD (not shown) staining. MZ area is shown by white line. Background fluorescence (grey box) was calculated and subtracted from MFI.

MATERIALS AND METHODS

Reagents, antibodies and oligonucleotides. This information is provided in **Supplementary Tables 7** (reagents), **8** (antibodies) and **9** (oligonucleotides).

Mouse strains and animal procedures. Mice on the C57BL/6 background used in this study were derivatives of the following: Tg(CD2-cre)4Kio[28], CD79a$^{tm1(cre)Reth}$[58], Tg(Fcer2a-cre)5Mbu[29], Gt(ROSA)26Sor$^{tm1(cre/ERT2)Thl}$ [59], Zfp36^{tm1Tnr} (**Supplementary Fig. 1**), Zfp36l1$^{tm1.1Tnr}$[26], Zfp36l2$^{tm1.1Tnr}$[26], Gt(Rosa)26Sor$^{tm1(GFPZfp36l1)Tnr}$ [27], B6.129S1-*Bcl2l11*$^{tm1.1Ast}$/J[60]. All mice were aged between 8-12 weeks. B6.SJL mice, which were used in competitive bone marrow chimera experiments, are Ly5.1 (CD45.1 allotype) C57BL/6 congenic mice obtained from Jackson labs, USA. For bone marrow chimeras, B6.SJL recipient mice were irradiated and reconstituted with a total of $3x10^6$ donor bone marrow cells by i.v. injection. Reconstituted mice were fed neomycin sulphate (Sigma) in their drinking water for four weeks post-reconstitution, and were analysed after 8-10 weeks. In the case of μMT chimeras, of the $3x10^6$ donor BM cells, 80% were taken from μMT mice, and 20% from either *Zfp36l1*$^{fl/fl}$ERT2$^{cre/+}$ or ERT2$^{cre/+}$controls. BrdU (Sigma) was administered at 0.8mg/ml in drinking water. Unless otherwise stated, control mice used in experiments were littermate controls that were negative for Cre. Tamoxifen (Cambridge Bioscience Ltd.) was prepared in sunflower oil containing 10% ethanol to a final concentration of 50mg/ml. Daily dosage for mice was 200mg/kg. Tamoxifen was fed to mice for two consecutive days using a bulb-tipped reusable feeding needle. After induction of cre, mice were returned to stock and euthanized at the appropriate time point. 0.8μg of PE-labelled anti-mouse CD19 antibody in PBS was administered intravenously and mice were culled at 5 minutes following injection. Spleen cell suspensions were prepared and surface stained as described. The Animal Welfare and Experimentation Committee of Babraham Institute and the UK Home Office approved all animal procedures at the Babraham Institute.

Flow cytometry. B cell populations were analysed using antibodies against B220, CD19, CD21, CD23, CD93, IgD and IgM (**Supplementary table 8**). B cells analysed in the bone marrow were as follows: Immature B cells, B220$^+$IgM$^+$IgD$^-$; Recirculating B cells, B220$^+$IgM$^-$ IgD$^+$. B cells analysed in the spleen were as follows: T1 B cells, B220$^+$CD93$^+$CD23$^-$IgM^{hi}; T2 B cells, B220$^+$CD93$^+$CD23$^+$IgM^{hi}; T3 B cells, B220$^+$CD93$^+$CD23$^+$IgM$^+$; marginal zone precursors, B220$^+$CD93$^+$CD21^{hi}IgM^{hi}; marginal zone B cells, B220$^+$CD93$^-$CD21^{hi}CD23$^-$ or B220$^+$CD9$^+$CD1d^{hi} and follicular B cells, B220$^+$CD93$^-$CD21$^+$CD23$^+$. Fixable viability dye eFluor780 was used to assess cell viability. BrdU was detected using the BrdU flow kit (BD), following the manufacturer's instructions. Cells were analysed using a BD LSRFortessa flow

cytometer. To measure apoptosis, $5x10^6$ cells were stained intracellularly with a FITC conjugated rabbit monoclonal antibody, which recognises active Caspase-3 (BD Biosciences).

Calcium flux analysis. Splenocytes were loaded for 30min at 37^0C in the dark with 0.6µM Ca^{2+} indicator PBX (BD) in serum free DMEM (5-$10x10^6$ cells). Cells were then stained with surface antibodies at RT, and resuspended in serum free Hanks medium. Cells were pre-treated with 10mM EGTA for 1 minute if required, before being stimulated with 10µg/ml goat polyclonal α-IgM F'ab fragment (Jackson ImmunoResearch). Fluorescence emission (525nm) was measured using a 488nm laser and 530/30 filter on a BD LSRFortessa flow cytometer.

B cell purification and sorting. B cells from spleen or peripheral lymph nodes were isolated with a B cell Isolation Kit from Miltenyi Biotech. To purify specific B cell subsets, cells were subsequently sorted using a BD FACSAria III or a BD FACSAria Fusion, using staining described above.

DNA isolation, RNA extraction and RT-qPCR assays. Total RNA was extracted from purified B cells using TRIzol (LifeTech) or RNeasy Micro or Mini Kit (Qiagen). RNA was treated with DNase I before reverse transcription into cDNA. ZFP36 family expression was analysed using custom and commercially available TaqMan assays with specific primers (**Supplementary Table 9**). Expression of mRNA was calculated using a standard curve and normalised to the expression of β2M. Genomic DNA was extracted from purified B cells using Cell lysis solution (Qiagen) containing proteinase K (Roche). Protein was removed by salt precipitation, and the DNA was isolated using isopropanol. Relative abundance of ZFP36l1 exon 2 was analysed by quantitative PCR with specific primers (**Supplementary Table 9**), qPCR assays were performed with Platinum SYBR Green qPCR SuperMix (Life Technologies). Relative abundance of ZFP36l1 was calculated using the comparative threshold cycle (ΔΔCT) method and results were normalised to the expression of TBP.

Immunofluorescence. Spleens were frozen in OCT compound on dry-ice, and sectioned on the cryostat (7-10µm thick). Sections were air dried overnight, then fixed in ice cold acetone for 15 mins at 4˚C. Tissue sections were rehydrated in PBS for 10, and blocked in 5% NRS. Sections were stained in 5% NRS at 4˚C overnight in a humidified chamber to detect IgM and MOMA-1, or CD1d, IgD and MOMA-1. Slides were washed PBS, and mounted in ProLong Gold antifade reagent (Thermo Fischer). Images were acquired at x10 or ×20 magnification using a DeltaVision widefield fluorescence microscope (GE Healthcare). Images were quantified using Image-J software (NIH). MZ width was measured using Image-J software. At least 10 follicles per genotype were imaged, measurements were taken from the edge of MOMA-1^+ cells to the edge of $CD1d^+$ staining. A number of measurements were taken per

follicle to account for variability. CD1d MFI (-background) was calculated using Image-J (NIH). Follicular area was defined using MOMA-1 (CD169) staining. MFI was then calculated for this area (see **Supplementary Fig. 8e**). MZ area was defined as $CD1d^{+}$ area outside MOMA-1 and IgD staining (see **Supplementary Fig. 8e**). Background fluorescence was calculated and subtracted from MFI values for MZ and FO. Measurements were taken from 10 follicles from 2 $ERT2^{cre/+}$ chimeras, and 25 follicles from 2 *Zfp36l1*$^{fl/fl}$$ERT2^{cre/+}$ chimeras.

Library preparation and high-throughput sequencing. Sorted MZ or FO B cells from individual control mice were independently processed for RNA extraction. RNAseq libraries were obtained using a TruSeq Stranded mRNA Sample Prep Kit (Illumina) or SMARTer Ultra Low Input RNA v4 and SMARTer Low Input Library Prep Kit V2 (Clontech). Low input libraries were prepared and sequenced from total RNA at Aros Applied Biotechnology A/S. RNAseq libraries were sequenced using the HTSeq2000 (Illumina). 100bp single end or paired end sequencing was performed on all libraries.

Bioinformatics for RNAseq. Quality of sequencing data was analysed using FastQC (http://www.bioinformatics.babraham.ac.uk/projects/fastqc/). Reads were mapped to mouse genome (GRCm38) using Tophat2[61]. Reads aligning to genes were counted using htseq-count[62] and analysis of differentially expressed genes was performed using the DESeq2 (R/bioconductor package)[63]. Reads were visualised using Integrative Genomics Viewer (IGV)[64, 65]. Gene set enrichment analysis was performed using ToppGene[66] and the enriched GO biological processes were visualised using Revigo[57]. iCLIP data was analysed as previously described[27].

To analyse conservation of Zfp36l1 binding motif in its target genes, the 3'UTR sequence of selected gene in mouse was queried against synthenic sequences in eutherian mammals using Ensembl Perl API.

Bioinformatics for publically available data. ChIP-seq data for Klf2[37] and IRF8[35] and Affymetrix data for *Klf2*-deficient FO B cells[14] were downloaded from the Gene Expression Omnibus. The Affymetrix data was analysed using R/Bioconductor package affy[67]. Reads from ChIP-seq data were mapped to mouse genome (GRCm38) using Bowtie2[68] and peaks were called using MACS2[69]. Only reproducible peaks were considered. Peaks were visualised using IGV.

Statistical analysis. Mann-Whitney tests were performed for statistical analysis of non-sequencing data. Additional details regarding sample size and statistics used have been provided in the figure legends where relevant.

Accession number. The RNA-seq data are available in the Gene Expression Omnibus (GEO) database (http://www.ncbi.nlm.nih.gov/gds) under the accession number: GSE79632.

Supplementary table 1: Differentially expressed genes in Figure 4A

Differentially expressed genes (padj<0.01) when comparing MZ B cells from tamoxifen treated *Zfp36l1*$^{fl/fl}$ERT2$^{cre/+}$ and ERT2$^{cre/+}$ mice. A 1.5 fold change cut-off has been applied.

Supplementary table 2: Up regulated genes (padj<0.01) for GSEA showing iCLIP hits and AREs

Genes that are increased in expression (padj<0.01) when comparing MZ B cells from tamoxifen treated *Zfp36l1*$^{fl/fl}$ERT2$^{cre/+}$ and ERT2$^{cre/+}$ mice. Hits in iCLIP analysis and ARE found in the 3'UTR of the gene are indicated. An FDR rate of 0.05 was used for the iCLIP data.

Supplementary table 3: Down regulated genes (padj<0.01) for GSEA showing iCLIP hits and AREs

Genes that are decreased in expression (padj<0.01) when comparing MZ B cells from tamoxifen treated *Zfp36l1*$^{fl/fl}$ERT2$^{cre/+}$ and ERT2$^{cre/+}$ mice. Hits in iCLIP analysis and ARE found in the 3'UTR of the gene are indicated. An FDR rate of 0.05 was used for the iCLIP data.

Supplementary table 4: Differentially expressed genes in Figure 5A

Differentially expressed genes (padj<0.01, and subject to a 1.5 fold cut-off) when comparing *Zfp36l1*$^{fl/fl}$ERT2$^{cre/+}$ (KO) MZ B cells and ERT2$^{cre/+}$ control (WT) MZ B cells to wildtype FO B cell gene expression. Gene lists have been separated into each quadrant of the correlation dot plot. Zfp36l1 has been removed from this analysis.

Supplementary table 5: Differentially expressed genes in Figure 5B

Differentially expressed genes (padj<0.01, and subject to a 1.5 fold cut-off) when comparing *Rosa26*^{GFPZFP36L1}CD23$^{cre/+}$ (GFP) FO B cells and *Rosa26*^{GFPZFP36L1} control FO B cells to wildtype MZ B cell gene expression. Gene lists have been separated into each quadrant of the correlation dot plot. Zfp36l1 has been removed from this analysis.

Supplementary table 6: Differentially expressed genes in Figure 5C

Differentially expressed genes (padj<0.05) found in RNAseq analysis comparing MZ B cells from *Zfp36l1*$^{fl/fl}$ERT2$^{cre/+}$ to ERT2$^{cre/+}$ controls and RNAseq analysis comparing GFP-ZFP36L1 positive FO B cells to FO B cells from littermate controls. Gene lists have been separated into each quadrant of the correlation dot plot. Zfp36l1 has been removed from this analysis.

Supplementary table 7: List of reagents

Reagent	Source	Cat. Number	Application
B cell Isolation Kit	Miltenyi Biotec	130-090-862	B cell isolation
DMEM	Life Tech	41965	Calcium flux
Hanks Medium	Sigma Aldrich	H6648	Calcium flux
PBX Calcium Assay kit	BD Biosciences	640175	Calcium flux
Fixable Viability Dye eFluor® 780	eBioscience	65-0865-14	FC
BD Cytofix/Cytoperm™	BD Biosciences	554714	FC
FITC BrdU Flow Kit	BD Biosciences	559619	BrdU Assay
APC BrdU Flow Kit	BD Biosciences	552598	BrdU Assay
5-bromo-2-deoxyuridine	Sigma Aldrich	B-5002	BrdU Assay
Dimethyl sulfoxide	Sigma Aldrich	D2650	-
TRIzol® Reagent	Life Tech	15596-026	RNA
RNeasy Micro Kit	Qiagen	74004	RNA
RNeasy Mini Kit	Qiagen	74106	RNA
RNase free DNase	Qiagen	79254	RNA
Platinum® SYBR® Green qPCR SuperMix-UDG w/ROX	Life Tech	11744	qPCR
TruSeq Stranded mRNA Sample Prep Kit	Illumina	RS-122-2103	RNAseq
SMART-Seq v4 Ultra Low Input RNA Kit for Sequencing	Clontech	634888	RNAseq
SMARTer low input library prep kit v2	Clontech	634899	RNAseq
Cell lysis solution	Qiagen	158908	DNA work
Protein precipitation solution	Qiagen	158910	DNA work
Tamoxifen	Cambridge Bioscience	CAY13258	Tamoxifen
OCT compound	Thermo Scientific	12678646	IF
Prolong Gold Antifade Mountant	Thermo Scientific	P36934	IF
Acetone (99.8% for HPLC)	Fisher Scientific	10442631	IF

Supplementary table 8: List of antibodies

Antigen	Source	Isotype (Clone)	Application	Company
B220/CD45R	Rat	IgG2a (RA3-6B2)	FC	eBioscience
β7 integrin	Rat	IgG2a (FIB504)	FC	Biolegend
Caspase 3	Rabbit	IgG (C92-605)	FC	BD Bioscience
CD1d	Mouse	IgG2b (WTH-2)	FC	T. Herrmann
CD1d	Rat	IgG2b (1B1)	IF	Biolegend
CD169	Rat	IgG2a (MOMA-1)	IF	Serotec
CD19	Rat	IgG2a (6D5)	FC	BioLegend
CD19	Rat	IgG2a (1D3)	FC	eBioscience
CD21	Rat	IgG2b (7G6)	FC	BD Pharmingen
CD21	Rat	IgG2a (4E3)	FC	eBioscience
CD23	Rat	IgG2a (B3B4)	FC	BD Pharmingen
CD45.2	Mouse	IgG2a (104)	FC	eBioscience
CD62L	Rat	IgG2a (MEL-14)	FC	eBioscience
CD93	Rat	IgG2b (AA4.1)	FC	eBioscience
IgD	Rat	IgG2a (11-26)	FC	eBioscience
IgD	Rat	IgG2a (11-26c.2a)	IF	Biolegend
IgM	Rat	IgG2a (R6-60.2)	FC	BD Biosciences
IgM	Goat	Whole IgG	IF	Jackson ImmunoResearch
IgM – F(ab)2	Goat	Mouse specific	Cell activation	Jackson ImmunoResearch
KLF2	Mouse	IgG2b (665333)	FC	R&D Systems
MHC-II (I-A/I-E)	Rat	IgG2b (M5/114.15.2)	FC	eBiosciences
P27	Rabbit	IgG (Y236)	FC	Abcam
Rabbit Ig	Goat	Rabbit specific	FC	Jackson ImmunoResearch
Rabbit Ig	Goat	Rabbit specific	FC	Molecular Probes
ZFP36l1 (BRF1/2)	Rabbit	Polyclonal	iCLIP	Cell Signaling

Supplementary table 9: List of primers and Taqman assays for RT-qPCR

Primer pair name	Sequence	Comment
TBP (fwd)	GAATCGGTTTCCCAAATACTCAG	Normalisation
TBP (rev)	CAATCTTAAAATCGCAATAATCGC	
ZFP36l1 exon 2 (fwd)	CCTATCAGATGGAGAGGTGCTGTC	Deletion efficiency
ZFP36l1 exon 2 (rev)	TGTAGTTGAGCATCTTGTTACCCTGG	

Commercially available Taqman assays

Taqman assay name	Assay ID	Comment
B2M	Mm00437762_m1	Normalisation
ZFP36	Mm00457144_m1	Transcript abundance

Custom Taqman assays

Primer pair name	Sequence	Comment	Probe Sequence
ZFP36l1 (fwd)	CTTCACGACACACCAGATCCTAGT	Transcript abundance	(FAM) AACGCCCACGATGA (MGB)
ZFP36l1 (rev)	TGCTGTAGTTGAGCATCTTGTTACC		
ZFP36l2 (fwd)	ATGTCGACCACACTTCTGTCACC	Transcript abundance	(FAM) AGGGATTTCTCCGTCTTGC
ZFP36l2 (rev)	CTTCTTGTCCAGCATGTTGTTCAG		

REFERENCES

1. Cinamon, G., Zachariah, M.A., Lam, O.M., Foss, F.W., Jr. & Cyster, J.G. Follicular shuttling of marginal zone B cells facilitates antigen transport. *Nature immunology* **9**, 54-62 (2008).

2. Arnon, T.I., Horton, R.M., Grigorova, I.L. & Cyster, J.G. Visualization of splenic marginal zone B-cell shuttling and follicular B-cell egress. *Nature* **493**, 684-688 (2013).

3. Song, J. *et al.* Extracellular matrix of secondary lymphoid organs impacts on B-cell fate and survival. *Proc Natl Acad Sci U S A* **110**, E2915-E2924 (2013).

4. Simonetti, G. *et al.* IRF4 controls the positioning of mature B cells in the lymphoid microenvironments by regulating NOTCH2 expression and activity. *J Exp Med* **210**, 2887-2902 (2013).

5. Fasnacht, N. *et al.* Specific fibroblastic niches in secondary lymphoid organs orchestrate distinct Notch-regulated immune responses. *J Exp Med* **211**, 2265-2279 (2014).

6. Cerutti, A., Cols, M. & Puga, I. Marginal zone B cells: virtues of innate-like antibody-producing lymphocytes. *Nature reviews. Immunology* **13**, 118-132 (2013).

7. Pillai, S. & Cariappa, A. The follicular versus marginal zone B lymphocyte cell fate decision. *Nature reviews. Immunology* **9**, 767-777 (2009).

8. Martin, F. & Kearney, J.F. Marginal-zone B cells. *Nature reviews. Immunology* **2**, 323-335 (2002).

9. Srivastava, B., Quinn, W.J., Hazard, K., Erikson, J. & Allman, D. Characterization of marginal zone B cell precursors. *J Exp Med* **202**, 1225-1234 (2005).

10. Kleiman, E. *et al.* Distinct Transcriptomic Features are Associated with Transitional and Mature B-Cell Populations in the Mouse Spleen. *Frontiers in immunology* **6**, 30 (2015).

11. Tan, J.B. *et al.* Lunatic and manic fringe cooperatively enhance marginal zone B cell precursor competition for delta-like 1 in splenic endothelial niches. *Immunity* **30**, 254-263 (2009).

12. Witt, C.M., Won, W.J., Hurez, V. & Klug, C.A. Notch2 haploinsufficiency results in diminished B1 B cells and a severe reduction in marginal zone B cells. *J Immunol* **171**, 2783-2788 (2003).

13. Feng, J. *et al.* IFN regulatory factor 8 restricts the size of the marginal zone and follicular B cell pools. *J Immunol* **186**, 1458-1466 (2011).

14. Hart, G.T., Wang, X., Hogquist, K.A. & Jameson, S.C. Krüppel-like factor 2 (KLF2) regulates B-cell reactivity, subset differentiation, and trafficking molecule expression. *PNAS* **2**, 1-6 (2010).

15. Winkelmann, R. *et al.* B cell homeostasis and plasma cell homing controlled by Kruppel-like factor 2. *Proceedings of the National Academy of Sciences of the United States of America* **108**, 710-715 (2011).

16. Vu, T.T. *et al.* Impaired B Cell Development in the Absence of Kruppel-like Factor 3. *Journal of immunology* **187**, 5032-5042 (2011).

17. Clipson, A. *et al.* KLF2 mutation is the most frequent somatic change in splenic marginal zone lymphoma and identifies a subset with distinct genotype. *Leukemia* **29**, 1177-1185 (2015).

18. Turner, M., Galloway, A. & Vigorito, E. Noncoding RNA and its associated proteins as regulatory elements of the immune system. *Nature immunology* **15**, 484-491 (2014).

19. Belver, L., de Yebenes, V.G. & Ramiro, A.R. MicroRNAs prevent the generation of autoreactive antibodies. *Immunity* **33**, 713-722 (2010).

20. Kramer, N.J. *et al.* Altered lymphopoiesis and immunodeficiency in miR-142 null mice. *Blood* **125**, 3720-3730 (2015).

21. Sadri, N., Lu, J.Y., Badura, M.L. & Schneider, R.J. AUF1 is involved in splenic follicular B cell maintenance. *BMC immunology* **11**, 1 (2010).

22. Diaz-Munoz, M.D. *et al.* The RNA-binding protein HuR is essential for the B cell antibody response. *Nature immunology* (2015).

23. Yuan, J., Nguyen, C.K., Liu, X., Kanellopoulou, C. & Muljo, S.A. Lin28b reprograms adult bone marrow hematopoietic progenitors to mediate fetal-like lymphopoiesis. *Science* **335**, 1195-1200 (2012).

24. Zhou, Y. *et al.* Lin28b promotes fetal B lymphopoiesis through the transcription factor Arid3a. *J Exp Med* **212**, 569-580 (2015).

25. Brooks, S.a. & Blackshear, P.J. Tristetraprolin (TTP): Interactions with mRNA and proteins, and current thoughts on mechanisms of action. *Biochim Biophys Acta* **1829**, 666-679 (2013).

26. Hodson, D.J. *et al.* Deletion of the RNA-binding proteins ZFP36L1 and ZFP36L2 leads to perturbed thymic development and T lymphoblastic leukemia. *Nature immunology* **11**, 717-724 (2010).

27. Galloway, A. *et al.* RNA-binding proteins ZFP36L1 and ZFP36L2 promote cell quiescence. *Science* **352**, 453-459 (2016).

28. de Boer, J. *et al.* Transgenic mice with hematopoietic and lymphoid specific expression of Cre. *European journal of immunology* **33**, 314-325 (2003).

29. Kwon, K. *et al.* Instructive role of the transcription factor E2A in early B lymphopoiesis and germinal center B cell development. *Immunity* **28**, 751-762 (2008).

30. Bell, S.E. *et al.* The RNA binding protein Zfp36l1 is required for normal vascularisation and post-transcriptionally regulates VEGF expression. *Developmental dynamics : an official publication of the American Association of Anatomists* **235**, 3144-3155 (2006).

31. Stumpo, D.J. *et al.* Chorioallantoic fusion defects and embryonic lethality resulting from disruption of Zfp36L1, a gene encoding a CCCH tandem zinc finger protein of the Tristetraprolin family. *Mol Cell Biol* **24**, 6445-6455 (2004).

32. Vogel, K.U., Bell, L.S., Galloway, A., Ahlfors, H. & Turner, M. The RNA-Binding Proteins Zfp36l1 and Zfp36l2 Enforce the Thymic beta-Selection Checkpoint by Limiting DNA Damage Response Signaling and Cell Cycle Progression. *J Immunol* **197**, 2673-2685 (2016).

33. Oliver, A.M., Martin, F., Gartland, G.L., Carter, R.H. & Kearney, J.F. Marginal zone B cells exhibit unique activation, proliferative and immunoglobulin secretory responses. *European journal of immunology* **27**, 2366-2374 (1997).

34. Leadbetter, E.A. *et al.* NK T cells provide lipid antigen-specific cognate help for B cells. *Proceedings of the National Academy of Sciences of the United States of America* **105**, 8339-8344 (2008).

35. Grajales-Reyes, G.E. *et al.* Batf3 maintains autoactivation of Irf8 for commitment of a CD8alpha(+) conventional DC clonogenic progenitor. *Nature immunology* **16**, 708-717 (2015).

36. Winkelmann, R., Sandrock, L., Kirberg, J., Jack, H.M. & Schuh, W. KLF2--a negative regulator of pre-B cell clonal expansion and B cell activation. *PLoS One* **9**, e97953 (2014).

37. Yeo, J.C. *et al.* Klf2 Is an Essential Factor that Sustains Ground State Pluripotency. *Cell Stem Cell* **14**, 864-872 (2014).

38. Revilla, I.D.R. *et al.* The B-cell identity factor Pax5 regulates distinct transcriptional programmes in early and late B lymphopoiesis. *The EMBO journal* **31**, 3130-3146 (2012).

39. Keene, J.D. RNA regulons: coordination of post-transcriptional events. *Nature reviews. Genetics* **8**, 533-543 (2007).

40. Tan, F.E. & Elowitz, M.B. Brf1 posttranscriptionally regulates pluripotency and differentiation responses downstream of Erk MAP kinase. *Proceedings of the National Academy of Sciences of the United States of America* **111**, E1740-1748 (2014).

41. Kaymak, E. & Ryder, S.P. RNA recognition by the Caenorhabditis elegans oocyte maturation determinant OMA-1. *The Journal of biological chemistry* **288**, 30463-30472 (2013).

42. Farley, B.M. & Ryder, S.P. POS-1 and GLD-1 repress glp-1 translation through a conserved binding-site cluster. *Molecular biology of the cell* **23**, 4473-4483 (2012).

43. Tamburino, A.M., Ryder, S.P. & Walhout, A.J.M. A Compendium of Caenorhabditis elegans RNA Binding Proteins Predicts Extensive Regulation at Multiple Levels. *G3-Genes Genom Genet* **3**, 297-304 (2013).

44. Alles, M. *et al.* Leukocyte beta7 integrin targeted by Kruppel-like factors. *J Immunol* **193**, 1737-1746 (2014).

45. Hoek, K.L. *et al.* Follicular B cell trafficking within the spleen actively restricts humoral immune responses. *Immunity* **33**, 254-265 (2010).

46. Santio, N.M. *et al.* Pim Kinases Promote Migration and Metastatic Growth of Prostate Cancer Xenografts. *PLoS One* **10**, e0130340 (2015).

47. Grundler, R. *et al.* Dissection of PIM serine/threonine kinases in FLT3-ITD-induced leukemogenesis reveals PIM1 as regulator of CXCL12-CXCR4-mediated homing and migration. *J Exp Med* **206**, 1957-1970 (2009).

48. Lin, C.C. *et al.* IL-1-induced Bhlhe40 identifies pathogenic T helper cells in a model of autoimmune neuroinflammation. *J Exp Med* **213**, 251-271 (2016).

49. Hsiao, S.P. & Chen, S.L. Myogenic regulatory factors regulate M-cadherin expression by targeting its proximal promoter elements. *The Biochemical journal* **428**, 223-233 (2010).

50. Jain, M., Zhang, L., Patterson, E.E. & Kebebew, E. KIAA0101 is overexpressed, and promotes growth and invasion in adrenal cancer. *PLoS One* **6**, e26866 (2011).

51. Aranda, J.F. *et al.* MYADM regulates Rac1 targeting to ordered membranes required for cell spreading and migration. *Molecular biology of the cell* **22**, 1252-1262 (2011).

52. Aranda, J.F. *et al.* MYADM controls endothelial barrier function through ERM-dependent regulation of ICAM-1 expression. *Molecular biology of the cell* **24**, 483-494 (2013).

53. Devis, L. *et al.* Activated leukocyte cell adhesion molecule (ALCAM) is a marker of recurrence and promotes cell migration, invasion and metastasis in early stage endometrioid endometrial cancer. *J Pathol* (2016).

54. Nalvarte, I., Damdimopoulos, A.E., Ruegg, J. & Spyrou, G. The expression and activity of thioredoxin reductase 1 splice variants v1 and v2 regulate the expression of genes associated with differentiation and adhesion. *Biosci Rep* **35** (2015).

55. Saito, T. *et al.* Notch2 Is Preferentially Expressed in Mature B Cells and Indispensible for Marginal Zone B Lineage Development. *Immunity* **18**, 675-685 (2003).

56. Reginato, M.J. *et al.* Integrins and EGFR coordinately regulate the pro-apoptotic protein Bim to prevent anoikis. *Nature cell biology* **5**, 733-740 (2003).

57. Supek, F., Bosnjak, M., Skunca, N. & Smuc, T. REVIGO summarizes and visualizes long lists of gene ontology terms. *PLoS One* **6**, e21800 (2011).

58. Hobeika, E. *et al.* Testing gene function early in the B cell lineage in mb1-cre mice. *Proceedings of the National Academy of Sciences of the United States of America* **103**, 13789-13794 (2006).

59. de Luca, C. *et al.* Complete rescue of obesity, diabetes, and infertility in db/db mice by neuron-specific LEPR-B transgenes. *The Journal of clinical investigation* **115**, 3484-3493 (2005).

60. Bouillet, P. *et al.* Proapoptotic Bcl-2 relative Bim required for certain apoptotic responses, leukocyte homeostasis, and to preclude autoimmunity. *Science* **286**, 1735-1738 (1999).

61. Kim, D. *et al.* TopHat2: accurate alignment of transcriptomes in the presence of insertions, deletions and gene fusions. *Genome biology* **14**, R36 (2013).

62. Anders, S., Pyl, P.T. & Huber, W. HTSeq--a Python framework to work with high-throughput sequencing data. *Bioinformatics* **31**, 166-169 (2015).

63. Love, M.I., Huber, W. & Anders, S. Moderated estimation of fold change and dispersion for RNA-seq data with DESeq2. *Genome biology* **15**, 550 (2014).

64. Robinson, J.T. *et al.* Integrative genomics viewer. *Nature biotechnology* **29**, 24-26 (2011).

65. Thorvaldsdottir, H., Robinson, J.T. & Mesirov, J.P. Integrative Genomics Viewer (IGV): high-performance genomics data visualization and exploration. *Brief Bioinform* **14**, 178-192 (2013).

66. Chen, J., Bardes, E.E., Aronow, B.J. & Jegga, A.G. ToppGene Suite for gene list enrichment analysis and candidate gene prioritization. *Nucleic acids research* **37**, W305-311 (2009).

67. Gautier, L., Cope, L., Bolstad, B.M. & Irizarry, R.A. affy--analysis of Affymetrix GeneChip data at the probe level. *Bioinformatics* **20**, 307-315 (2004).

68. Langmead, B., Trapnell, C., Pop, M. & Salzberg, S.L. Ultrafast and memory-efficient alignment of short DNA sequences to the human genome. *Genome biology* **10**, R25 (2009).

69. Zhang, Y. *et al.* Model-based analysis of ChIP-Seq (MACS). *Genome biology* **9**, R137 (2008).

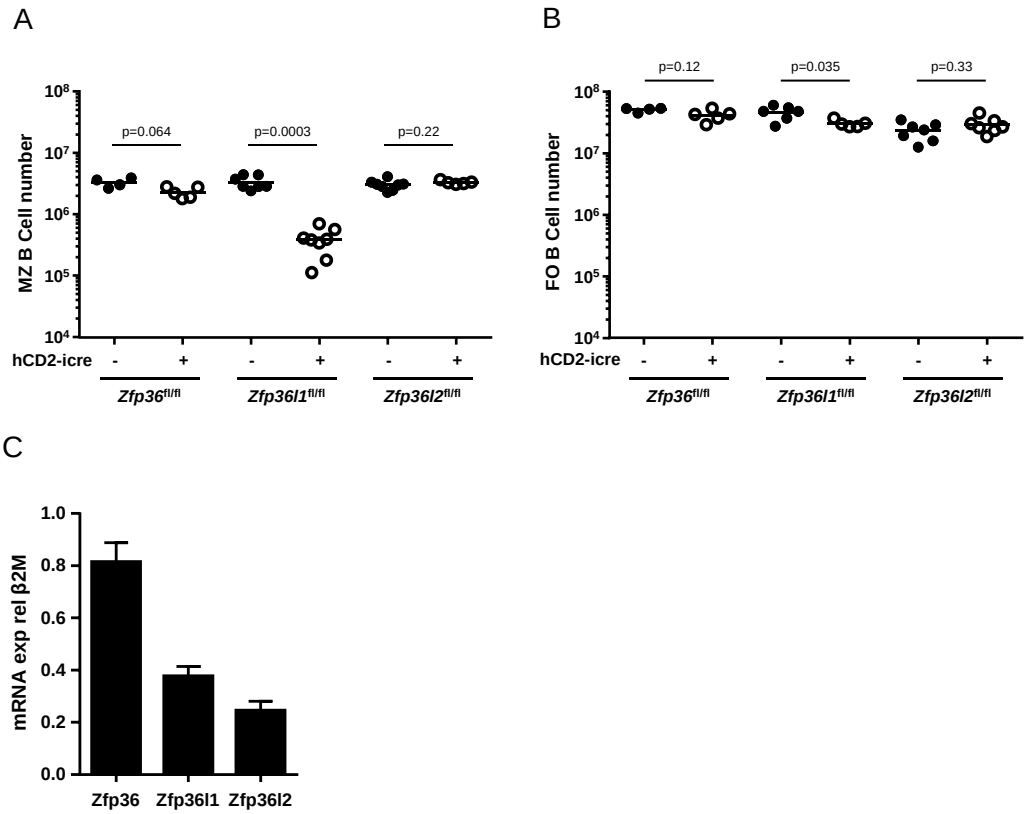
A
MZ B Cell number
10^8
10^7
10^6
10^5
10^4
p=0.064
p=0.0003
p=0.22
hCD2-icre
-
+
-
+
-
+
Zfp36fl/fl
Zfp36l1fl/fl
Zfp36l2fl/fl
B
FO B Cell number
p=0.12
p=0.035
p=0.33
C
mRNA exp rel β2M
1.0
0.8
0.6
0.4
0.2
0.0
Zfp36
Zfp36l1
Zfp36l2

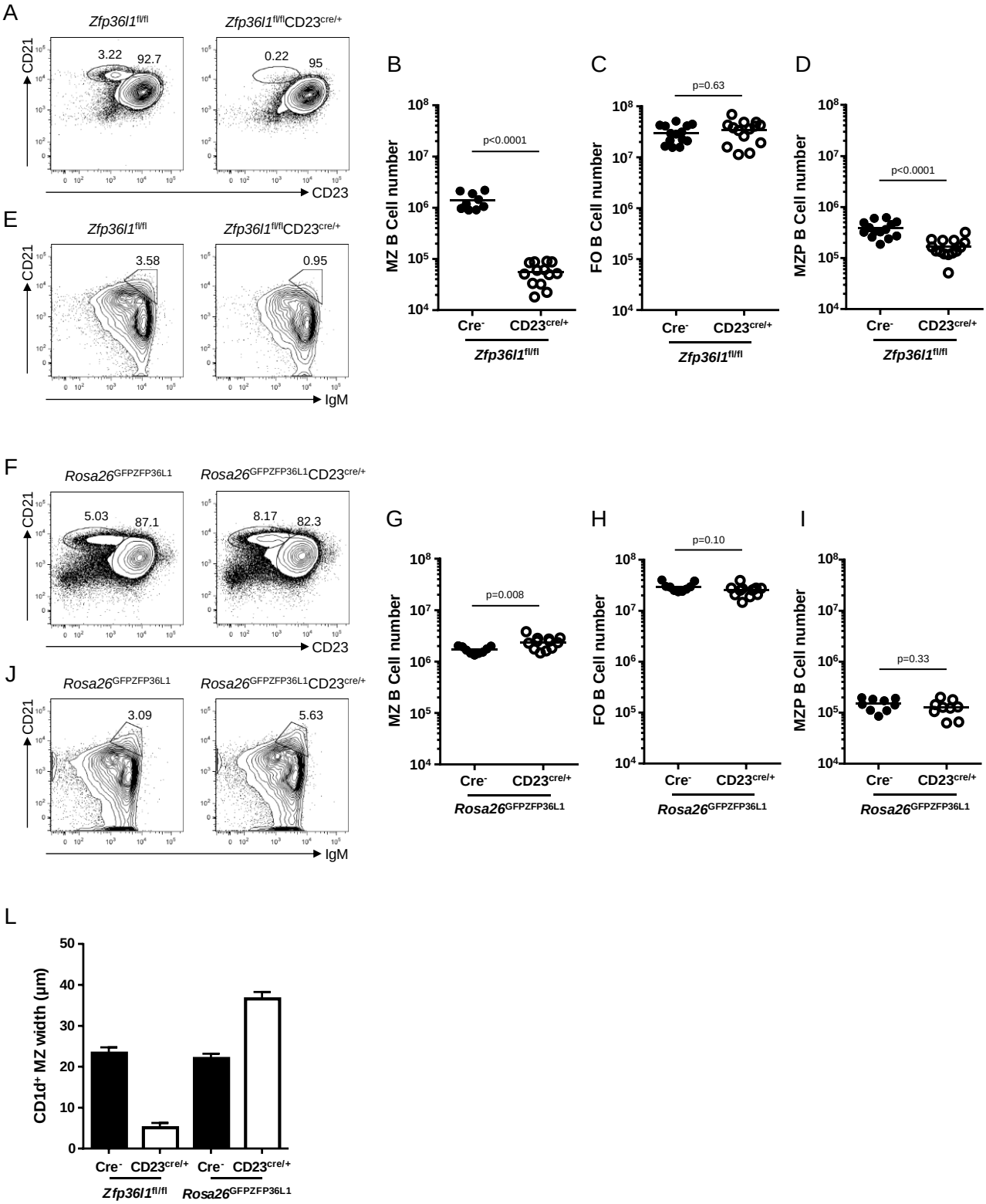
A
Zfp36l1fl/fl
Zfp36l1fl/flCD23cre/+
CD21
3.22
92.7
0.22
95
CD23
B
MZ B Cell number
p<0.0001
Cre-
CD23cre/+
Zfp36l1fl/fl
C
FO B Cell number
p=0.63
D
MZP B Cell number
p<0.0001
E
3.58
0.95
IgM
F
Rosa26GFPZFP36L1
Rosa26GFPZFP36L1CD23cre/+
5.03
87.1
8.17
82.3
G
p=0.008
H
p=0.10
I
p=0.33
J
3.09
5.63
L
CD1d+ MZ width (μm)
Rosa26GFPZFP36L1

K

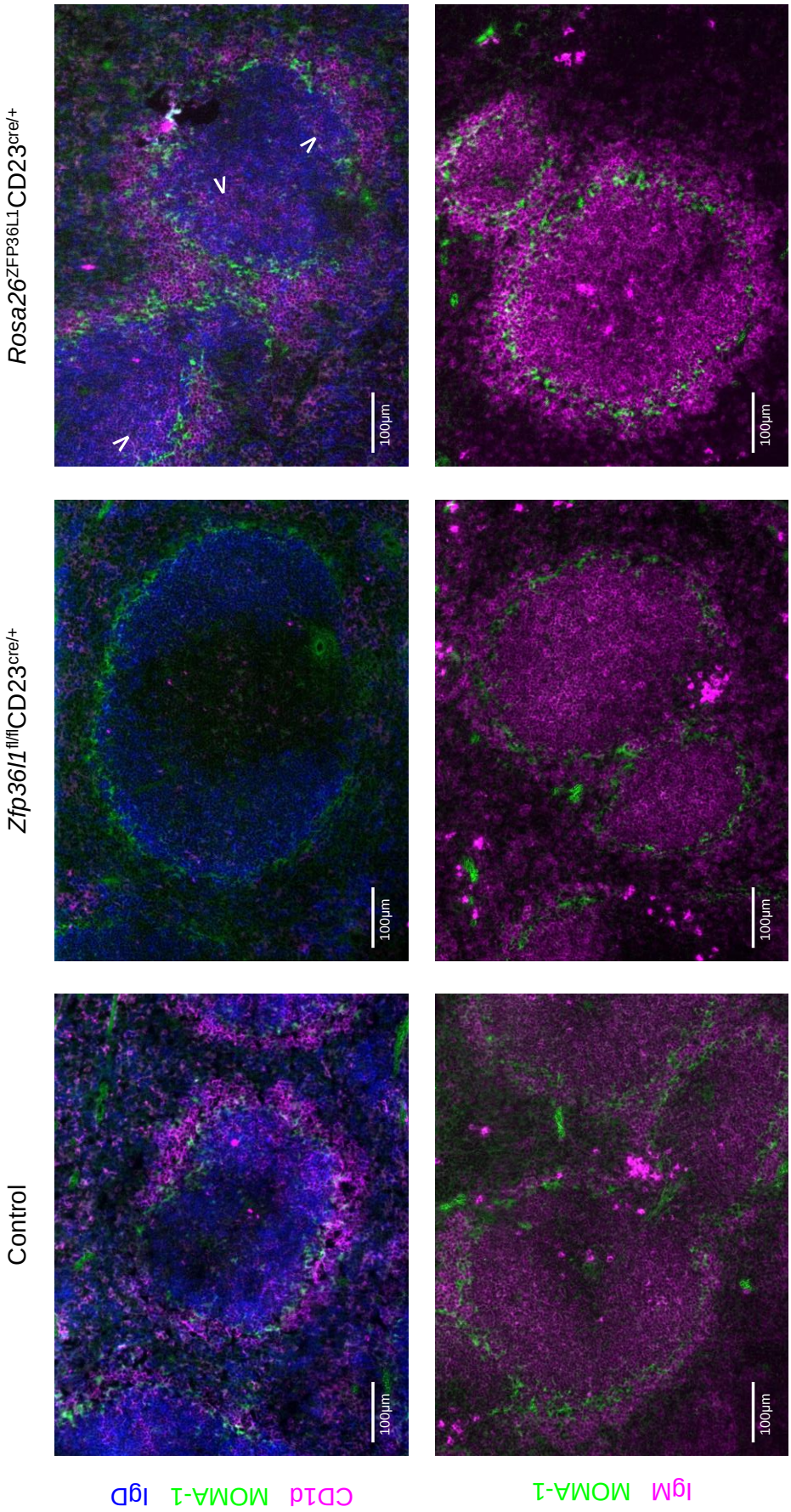
Rosa26ZFP36L1CD23cre/+
Zfp36l1fl/flCD23cre/+
Control
IgM MOMA-1
CD1d MOMA-1 IgD
100µm

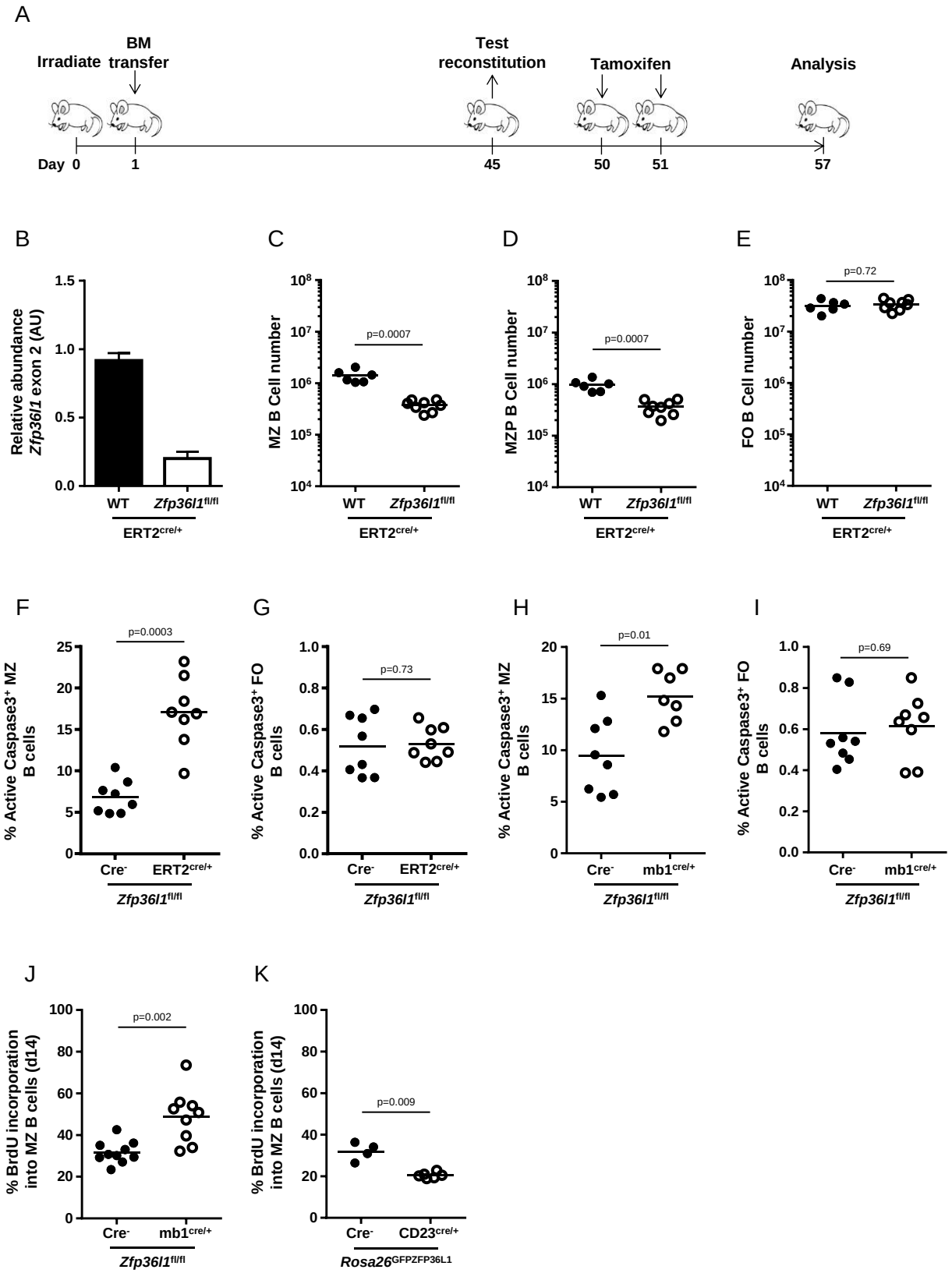
A
Irradiate
BM transfer
Test reconstitution
Tamoxifen
Analysis
Day 0
1
45
50
51
57
B
Relative abundance Zfp36l1 exon 2 (AU)
WT
Zfp36l1fl/fl
ERT2cre/+
C
MZ B Cell number
p=0.0007
D
MZP B Cell number
p=0.0007
E
FO B Cell number
p=0.72
F
% Active Caspase3+ MZ B cells
p=0.0003
Cre-
ERT2cre/+
Zfp36l1fl/fl
G
% Active Caspase3+ FO B cells
p=0.73
H
% Active Caspase3+ MZ B cells
p=0.01
mb1cre/+
I
% Active Caspase3+ FO B cells
p=0.69
J
% BrdU incorporation into MZ B cells (d14)
p=0.002
K
% BrdU incorporation into MZ B cells (d14)
p=0.009
CD23cre/+
Rosa26GFPZFP36L1

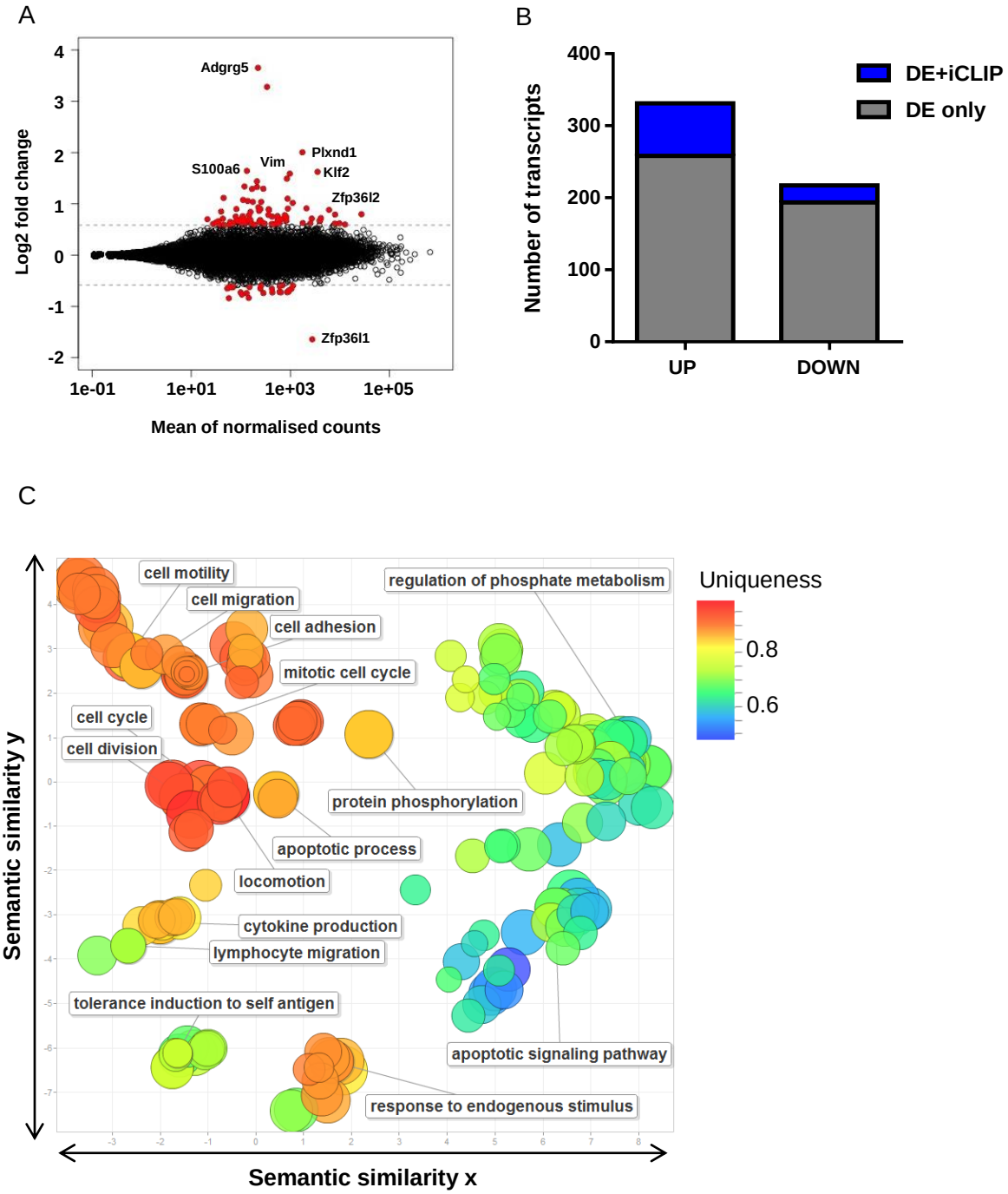
A
Log2 fold change
Mean of normalised counts
Adgrg5
Plxnd1
S100a6
Vim
Klf2
Zfp36l2
Zfp36l1
1e-01
1e+01
1e+03
1e+05
B
Number of transcripts
DE+iCLIP
DE only
UP
DOWN
C
Semantic similarity y
Semantic similarity x
Uniqueness
0.8
0.6
cell motility
cell migration
cell adhesion
mitotic cell cycle
cell cycle
cell division
regulation of phosphate metabolism
protein phosphorylation
apoptotic process
locomotion
cytokine production
lymphocyte migration
tolerance induction to self antigen
apoptotic signaling pathway
response to endogenous stimulus

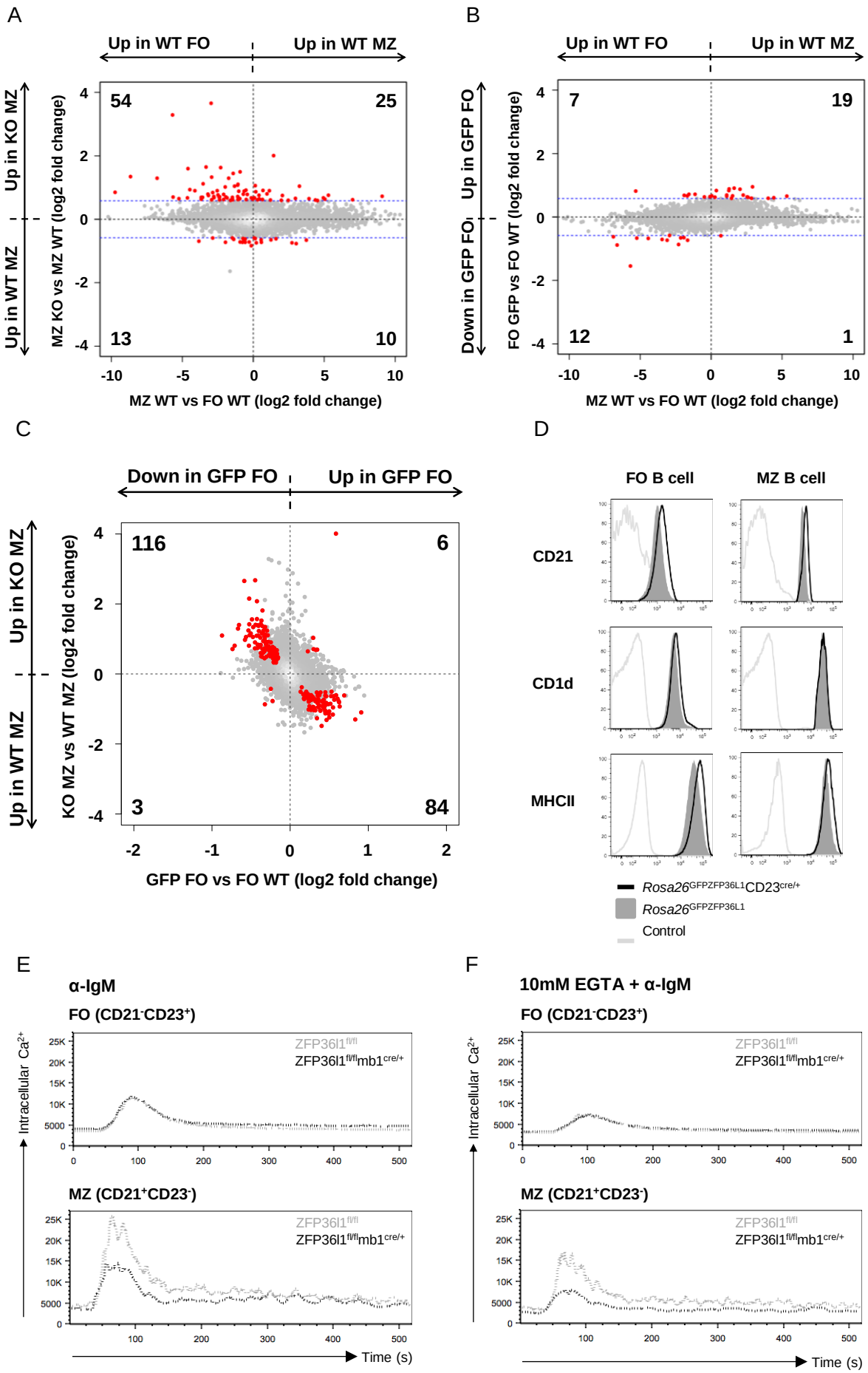
A
Up in WT FO
Up in WT MZ
Up in KO MZ
Up in WT MZ
MZ KO vs MZ WT (log2 fold change)
MZ WT vs FO WT (log2 fold change)
54
25
13
10
B
Up in WT FO
Up in WT MZ
Up in GFP FO
Down in GFP FO
FO GFP vs FO WT (log2 fold change)
MZ WT vs FO WT (log2 fold change)
7
19
12
1
C
Down in GFP FO
Up in GFP FO
Up in KO MZ
Up in WT MZ
KO MZ vs WT MZ (log2 fold change)
GFP FO vs FO WT (log2 fold change)
116
6
3
84
D
FO B cell
MZ B cell
CD21
CD1d
MHCII
Rosa26GFPZFP36L1CD23cre/+
Rosa26GFPZFP36L1
Control
E
α-IgM
FO (CD21-CD23+)
MZ (CD21+CD23-)
Intracellular Ca2+
ZFP36l1fl/fl
ZFP36l1fl/flmb1cre/+
Time (s)
F
10mM EGTA + α-IgM
FO (CD21-CD23+)
MZ (CD21+CD23-)
Intracellular Ca2+
ZFP36l1fl/fl
ZFP36l1fl/flmb1cre/+
Time (s)

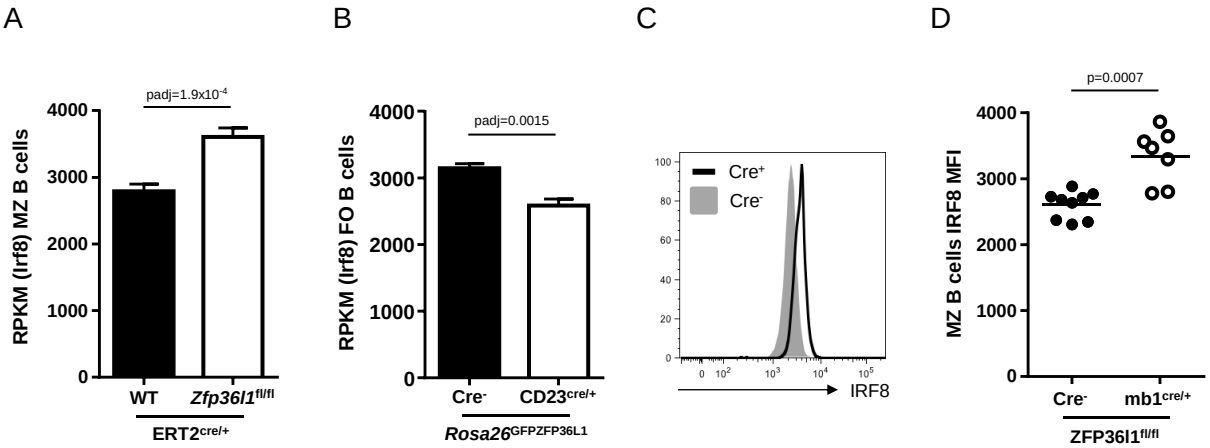

E

```
Mouse                8:120755170-120756700    CTAGTGT---------------CCAAATATTTATTTTTGTATTCTCTTAAGAAGTAT----
Cow                  18:11904197-11921287     -TAATATGCTGA----------AA----AACTATTTTTTGATTTCATTAAAA-AGTTTACTA
Dog                  5:66789257-66791355      -GAATATGCTAA----------ATGAATATTTATTTTTGTATCCATTTAAAATGTATA---
Horse                3:32873474-32875681      -TAATATGCTGA----------ATGAATATTTATTTTTGTATCCATTTAAGAAATATG---
Green Monkey         5:71324280-71325628      -TAATATGCTGA----------ATGAATATTTATTTTTGCATCCATTT--ACAGTATA---
Rhesus Macaque       20:84072219-84073569     -TAATATGCTGA----------ATGAATATTTATTTTTGTATCCATTT--ACAGTATA---
Olive Baboon         20:67654959-67656621     -TAATATGCTGA----------ATGAATATTTATTTTTGTACCCATTT--ACAGTATA---
Orangutan            16:73662315-73663670     -TAATATGCTGA----------ATGAATATTTATTTTTGTATCCATTAAAACAGTATA---
Gorilla              16:76499697-76501051     -TAATATGCTGA----------ATGAATATTTATTTTTGTATCCATTAAAACAGTGTA---
Human                16:85921277-85922613     -TAATATGCTGA----------ATGAATATTTATTTTTGTATCCATTAAAACAGTATA---
Chimpanzee           16:85584657-85586011     -TAATATGCTGA----------ATGAATATTTATTTTTGTATCCATTAAAACAGTATA---
Marmoset             20:40326666-40328352     -TAATATGCTGA----------GTGAATATTTATTTTTGTATCCATTAAAACGGTATA---
Rat                  19:65053991-65055536     CAAGTGTGCCCAACTCTGTAATCCAAATATTTATTTTTGTATTCACTTAAAAAGTAT----
Rabbit               GL019024:192070-193370   -CACCGTGCCGA----------GC-GGTATTTATTTTTGTAGCAGTTTTAAAAGTATC---
                                                *  .*                  *: ******** : .   *:  .  .* *
                                                                 ARE: TATTTATTTTT
                                                                 iCLIP: TATTTATTTTT
```

F

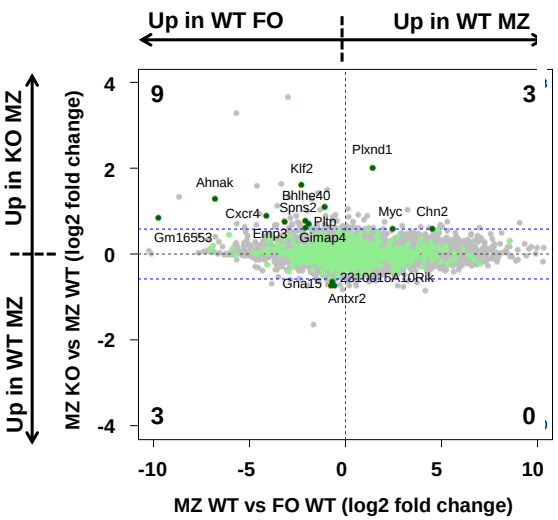

G

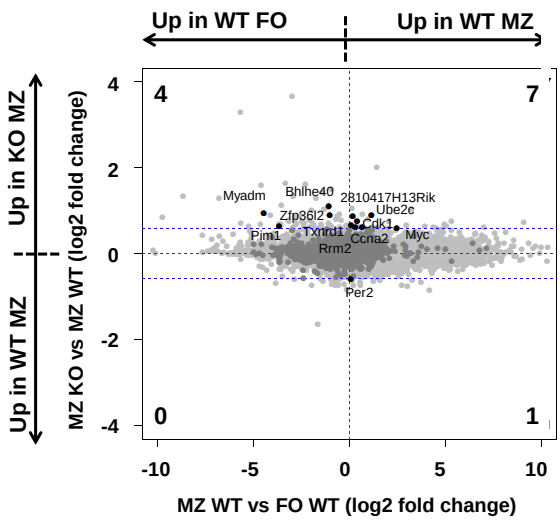

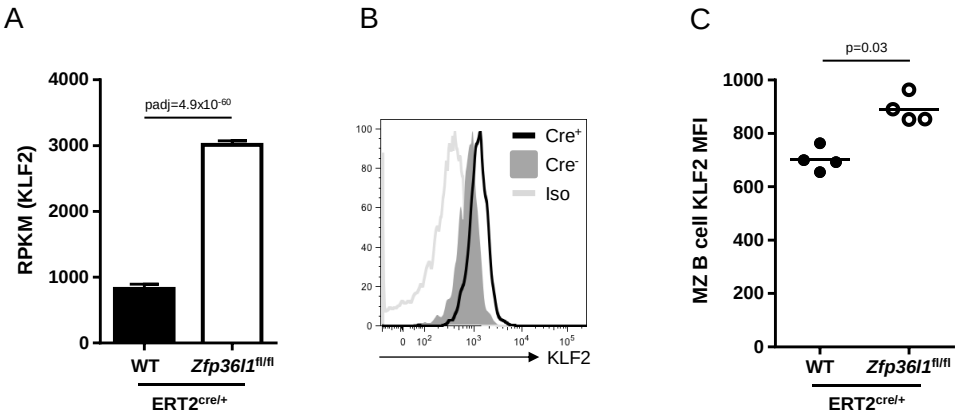

D

```
Human       19:16327014-16327876  GCGGCCCCCTCCCAAAC-TGTGACTGGTATTTATTGGACCCAGAGAACCGGGCCGGGCACA
Gorilla     19:16635703-16636556  GCGGCCCCCTCCCAAAC-TGTGACTGGTATTTATTGGACCCAGAGAACCGGGCCGGGCACA
Mouse       8:72320917-72321659   ACGGTCCCCTTGCAAACAGACTGC---TATTTATTGGACC-TTAGGACAGAGCCGGACAAG
Rat         16:19083527-19084198  ACGGCCCCCTTGCAACAAACTGACTGTTATTTATTGGACCCTGAGGACGGAGTCGGACAAG
                                   *** *****  ***        *   ************* * ** ** * * *** **

                                                ARE: TATTTATT
                                              iCLIP: TATTTATT
```

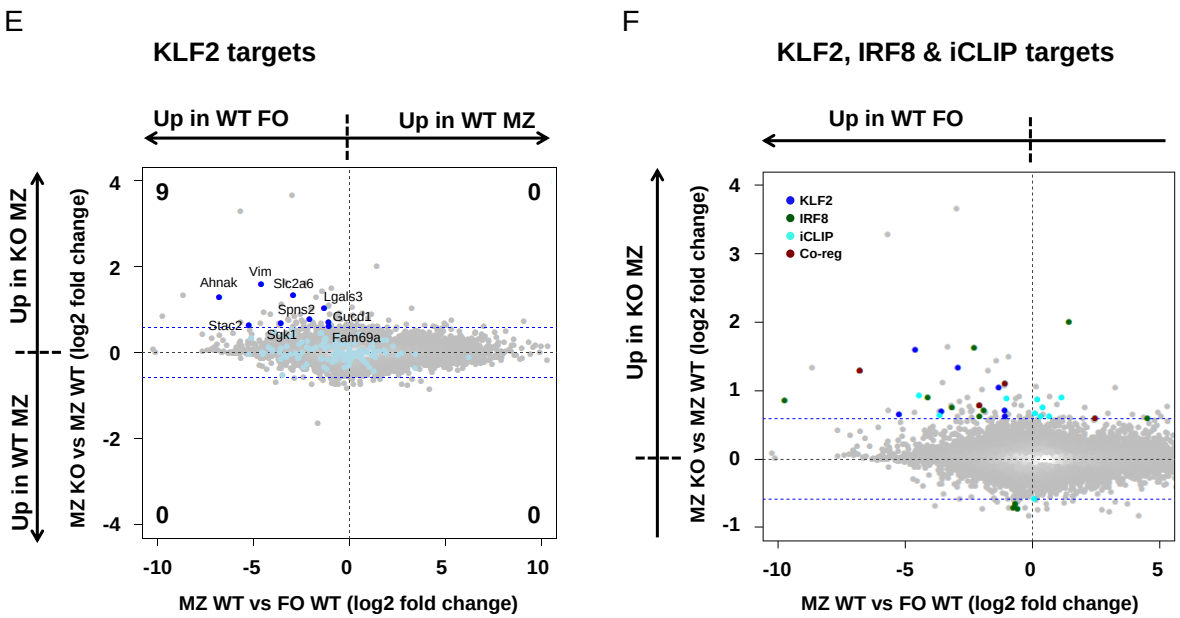

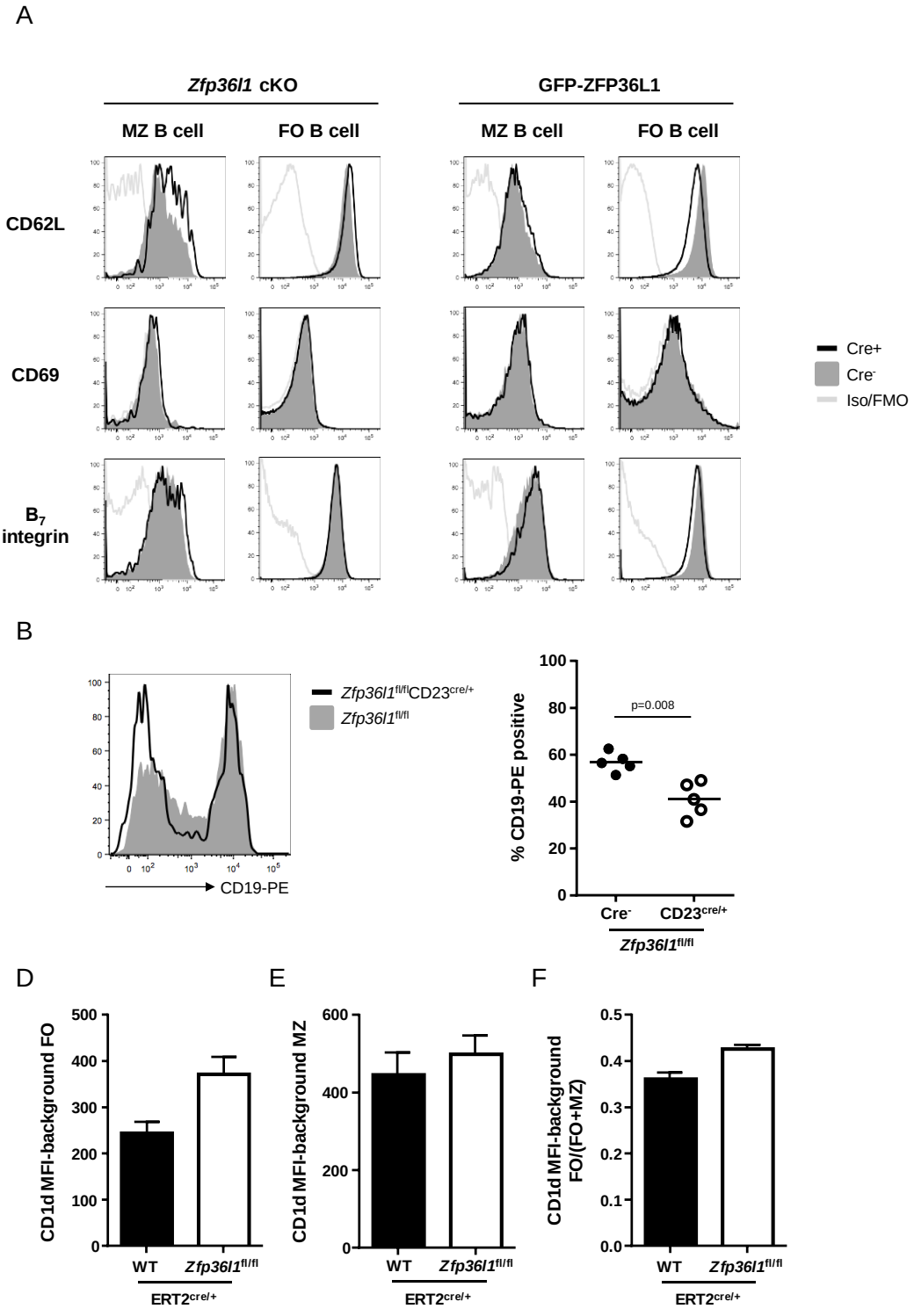
A
Zfp36l1 cKO
GFP-ZFP36L1
MZ B cell
FO B cell
MZ B cell
FO B cell
CD62L
CD69
B7 integrin
Cre+
Cre-
Iso/FMO
B
Zfp36l1fl/flCD23cre/+
Zfp36l1fl/fl
CD19-PE
% CD19-PE positive
p=0.008
Cre-
CD23cre/+
Zfp36l1fl/fl
D
CD1d MFI-background FO
WT
Zfp36l1fl/fl
ERT2cre/+
E
CD1d MFI-background MZ
WT
Zfp36l1fl/fl
ERT2cre/+
F
CD1d MFI-background FO/(FO+MZ)
WT
Zfp36l1fl/fl
ERT2cre/+

C

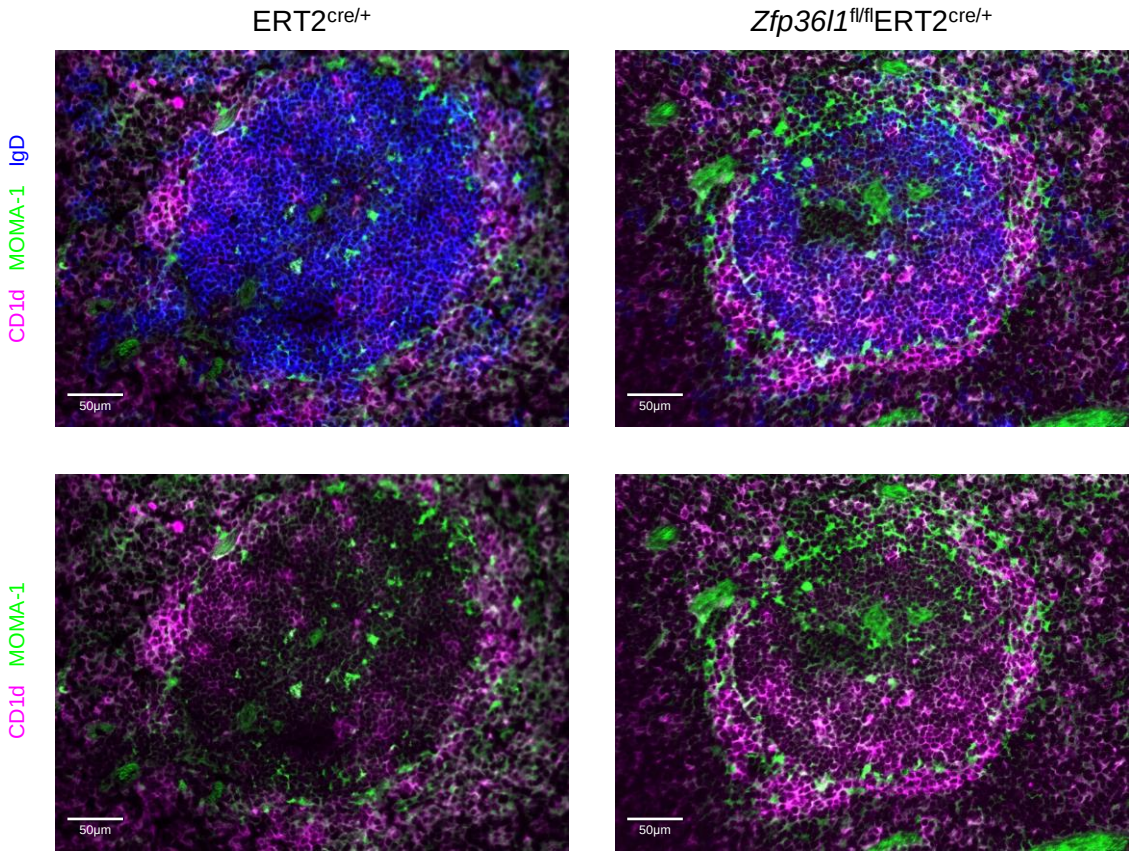
ERT2cre/+
Zfp36l1fl/flERT2cre/+
CD1d MOMA-1 IgD
CD1d MOMA-1
50μm
50μm
50μm
50μm

A

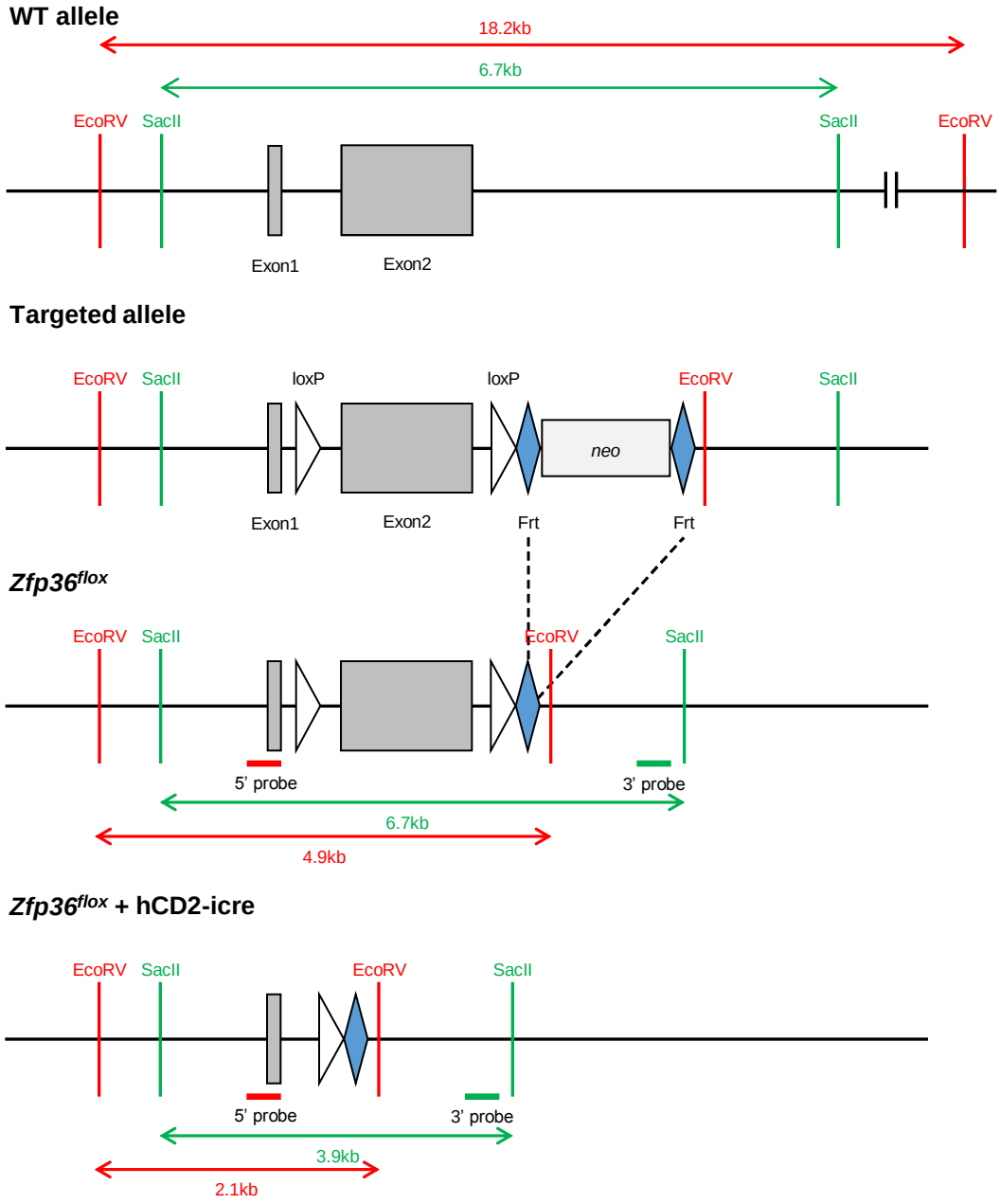
WT allele
18.2kb
6.7kb
EcoRV
SacII
SacII
EcoRV
Exon1
Exon2
Targeted allele
EcoRV
SacII
loxP
loxP
EcoRV
SacII
neo
Exon1
Exon2
Frt
Frt
Zfp36flox
EcoRV
SacII
EcoRV
SacII
5' probe
3' probe
6.7kb
4.9kb
Zfp36flox + hCD2-icre
EcoRV
SacII
EcoRV
SacII
5' probe
3' probe
3.9kb
2.1kb

B

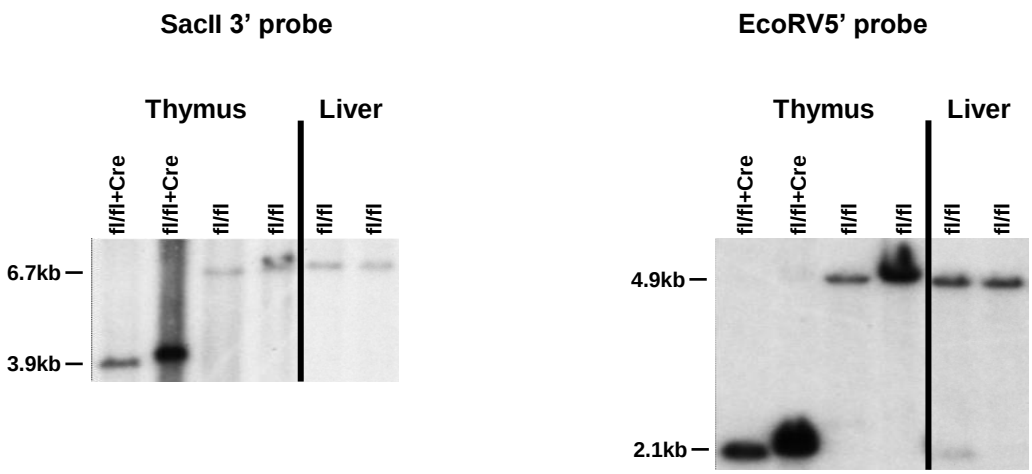
SacII 3' probe
Thymus
Liver
fl/fl+Cre
fl/fl+Cre
fl/fl
fl/fl
fl/fl
fl/fl
6.7kb
3.9kb
EcoRV5' probe
Thymus
Liver
fl/fl+Cre
fl/fl+Cre
fl/fl
fl/fl
fl/fl
fl/fl
4.9kb
2.1kb

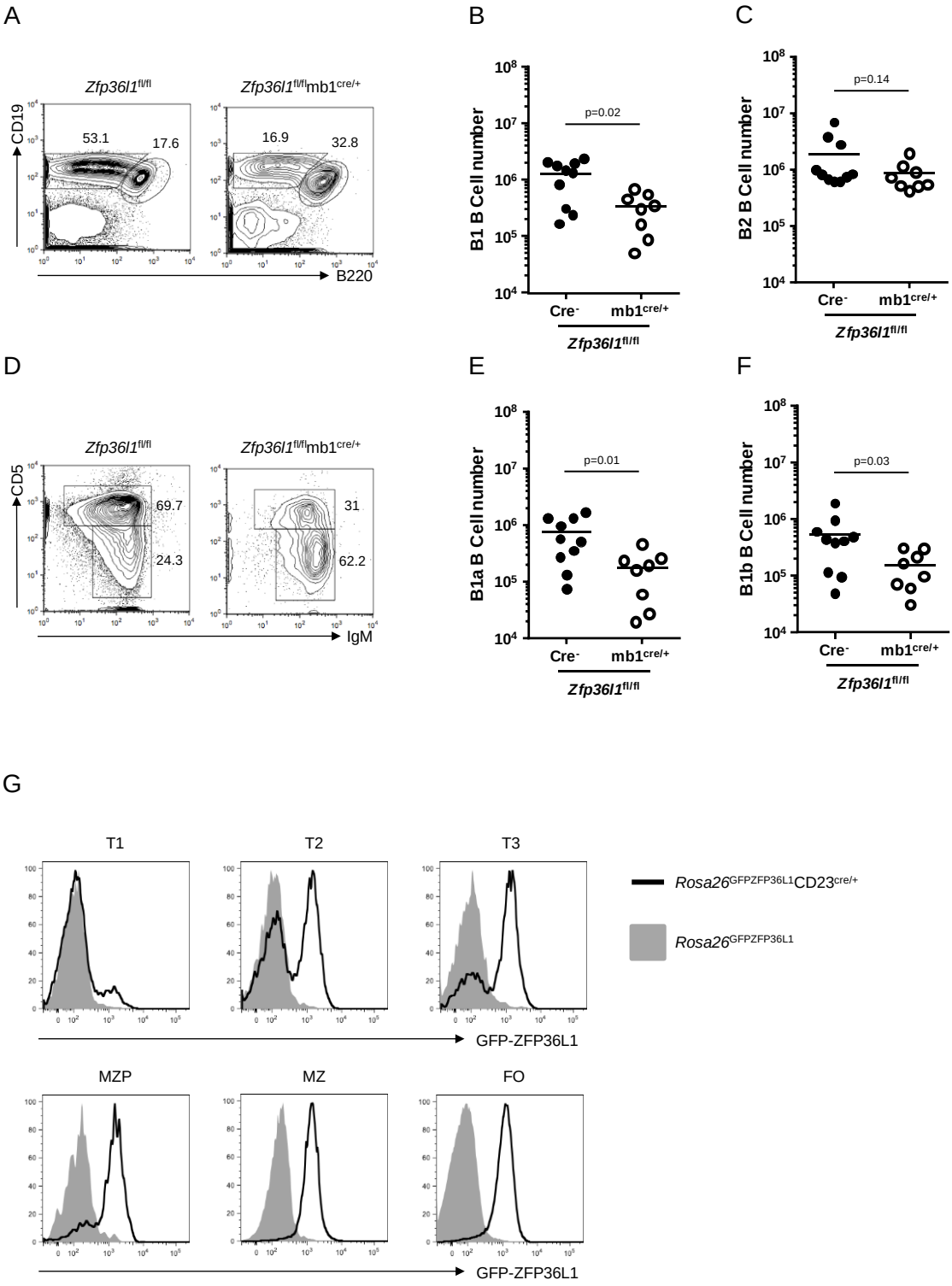
A
Zfp36l1fl/fl
Zfp36l1fl/flmb1cre/+
CD19
53.1
17.6
16.9
32.8
B220
B
B1 B Cell number
p=0.02
Cre-
mb1cre/+
Zfp36l1fl/fl
C
B2 B Cell number
p=0.14
Cre-
mb1cre/+
Zfp36l1fl/fl
D
Zfp36l1fl/fl
Zfp36l1fl/flmb1cre/+
CD5
69.7
24.3
31
62.2
IgM
E
B1a B Cell number
p=0.01
Cre-
mb1cre/+
Zfp36l1fl/fl
F
B1b B Cell number
p=0.03
Cre-
mb1cre/+
Zfp36l1fl/fl
G
T1
T2
T3
Rosa26GFPZFP36L1CD23cre/+
Rosa26GFPZFP36L1
GFP-ZFP36L1
MZP
MZ
FO
GFP-ZFP36L1

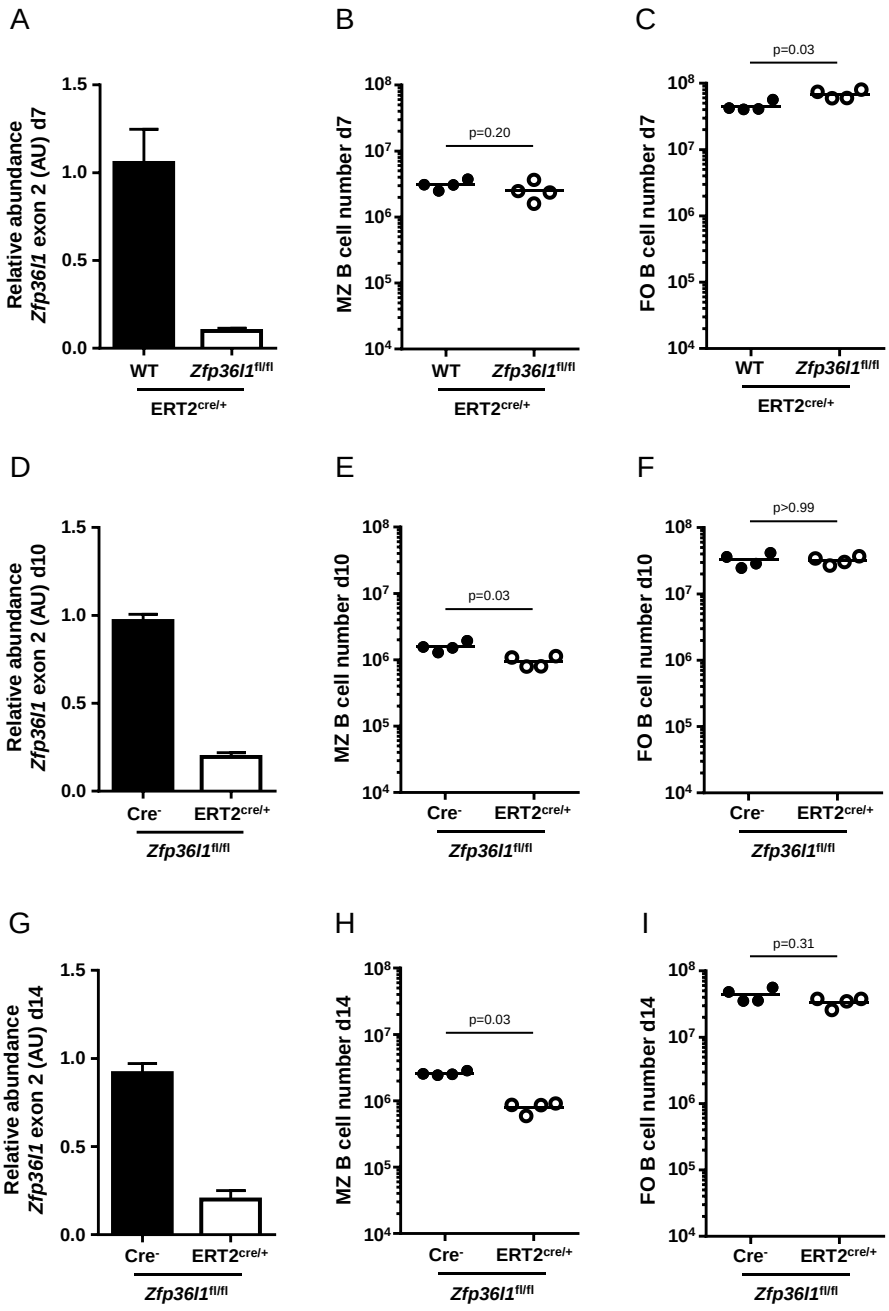
A
Relative abundance Zfp36l1 exon 2 (AU) d7
1.5
1.0
0.5
0.0
WT
Zfp36l1fl/fl
ERT2cre/+
B
MZ B cell number d7
p=0.20
WT
Zfp36l1fl/fl
ERT2cre/+
C
FO B cell number d7
p=0.03
WT
Zfp36l1fl/fl
ERT2cre/+
D
Relative abundance Zfp36l1 exon 2 (AU) d10
Cre-
ERT2cre/+
Zfp36l1fl/fl
E
MZ B cell number d10
p=0.03
Cre-
ERT2cre/+
Zfp36l1fl/fl
F
FO B cell number d10
p>0.99
Cre-
ERT2cre/+
Zfp36l1fl/fl
G
Relative abundance Zfp36l1 exon 2 (AU) d14
Cre-
ERT2cre/+
Zfp36l1fl/fl
H
MZ B cell number d14
p=0.03
Cre-
ERT2cre/+
Zfp36l1fl/fl
I
FO B cell number d14
p=0.31
Cre-
ERT2cre/+
Zfp36l1fl/fl

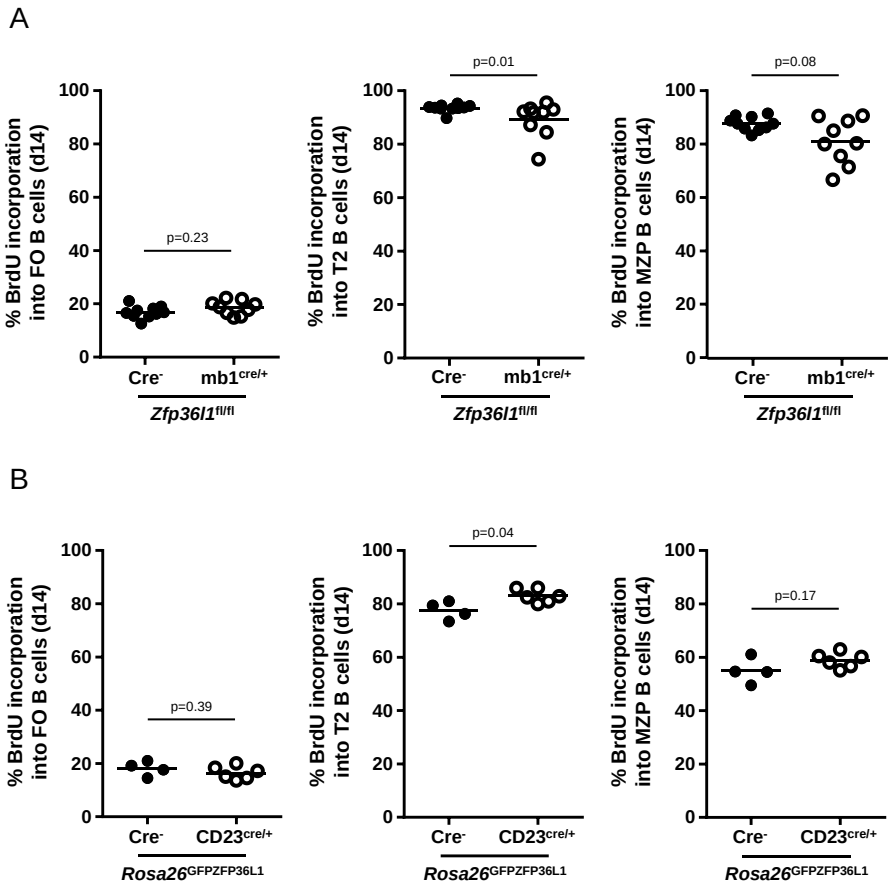
A
% BrdU incorporation into FO B cells (d14)
p=0.23
Cre-
mb1cre/+
Zfp36l1fl/fl
% BrdU incorporation into T2 B cells (d14)
p=0.01
Cre-
mb1cre/+
Zfp36l1fl/fl
% BrdU incorporation into MZP B cells (d14)
p=0.08
Cre-
mb1cre/+
Zfp36l1fl/fl
B
% BrdU incorporation into FO B cells (d14)
p=0.39
Cre-
CD23cre/+
Rosa26GFPZFP36L1
% BrdU incorporation into T2 B cells (d14)
p=0.04
Cre-
CD23cre/+
Rosa26GFPZFP36L1
% BrdU incorporation into MZP B cells (d14)
p=0.17
Cre-
CD23cre/+
Rosa26GFPZFP36L1

A

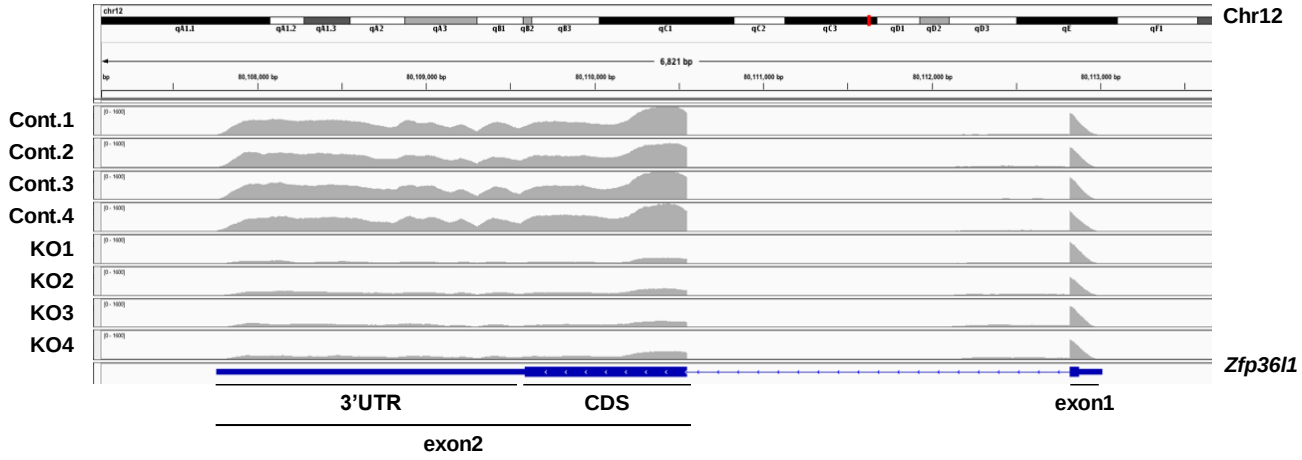
Chr12
Cont.1
Cont.2
Cont.3
Cont.4
KO1
KO2
KO3
KO4
Zfp36l1
3'UTR
CDS
exon1
exon2

B

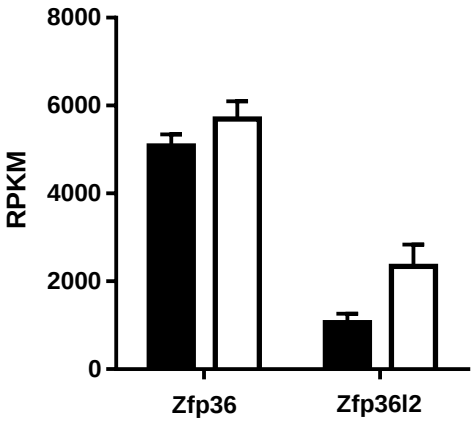
RPKM
8000
6000
4000
2000
0
Zfp36
Zfp36l2

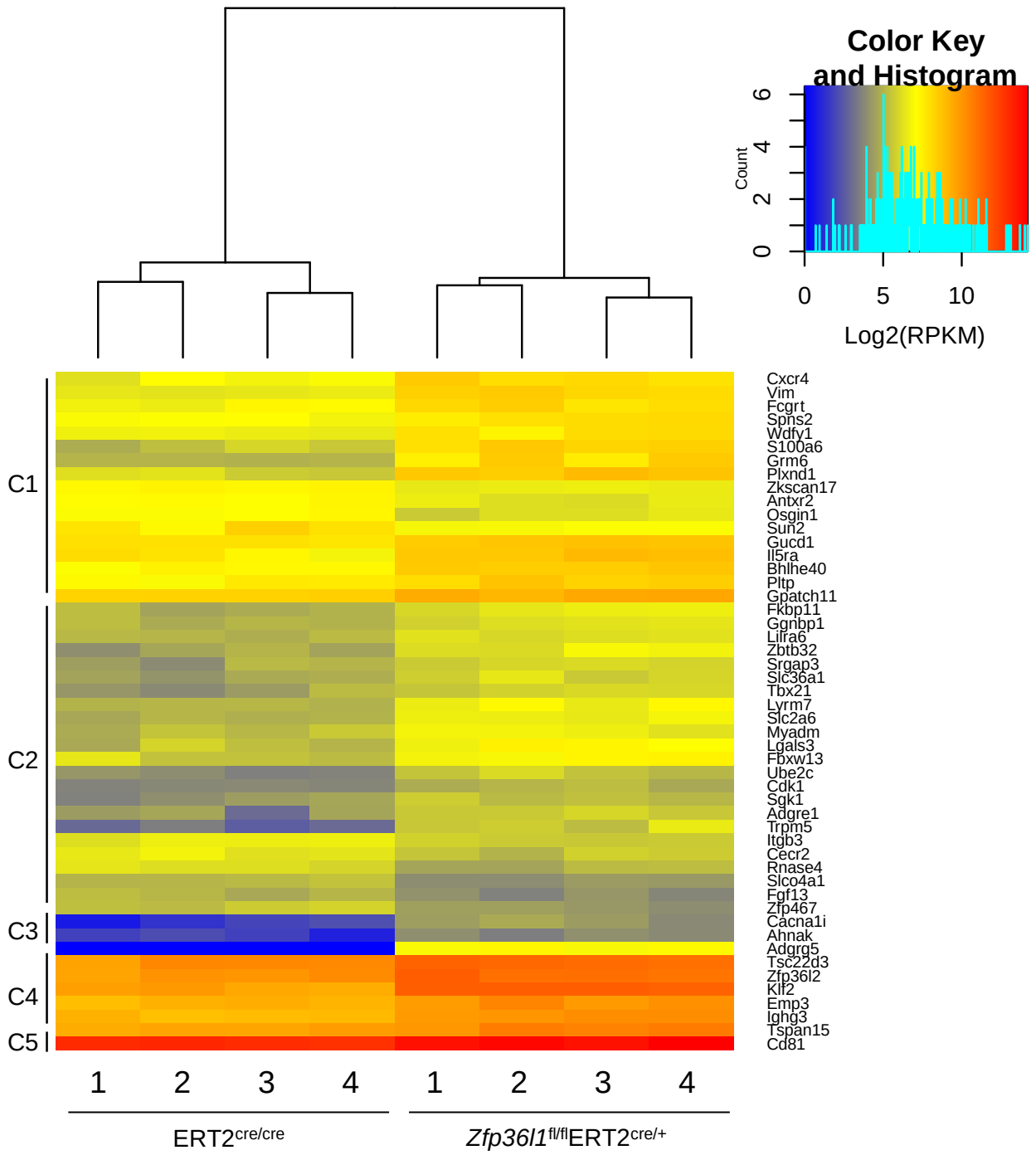
Color Key
and Histogram
Count
0
2
4
6
0
5
10
Log2(RPKM)
C1
C2
C3
C4
C5
Cxcr4
Vim
Fcgrt
Spns2
Wdfy1
S100a6
Grm6
Plxnd1
Zkscan17
Antxr2
Osgin1
Sun2
Gucd1
Il5ra
Bhlhe40
Pltp
Gpatch11
Fkbp11
Ggnbp1
Lilra6
Zbtb32
Srgap3
Slc36a1
Tbx21
Lyrm7
Slc2a6
Myadm
Lgals3
Fbxw13
Ube2c
Cdk1
Sgk1
Adgre1
Trpm5
Itgb3
Cecr2
Rnase4
Slco4a1
Fgf13
Zfp467
Cacna1i
Ahnak
Adgrg5
Tsc22d3
Zfp36l2
Klf2
Emp3
Ighg3
Tspan15
Cd81
1
2
3
4
1
2
3
4
ERT2cre/cre
Zfp36l1fl/flERT2cre/+

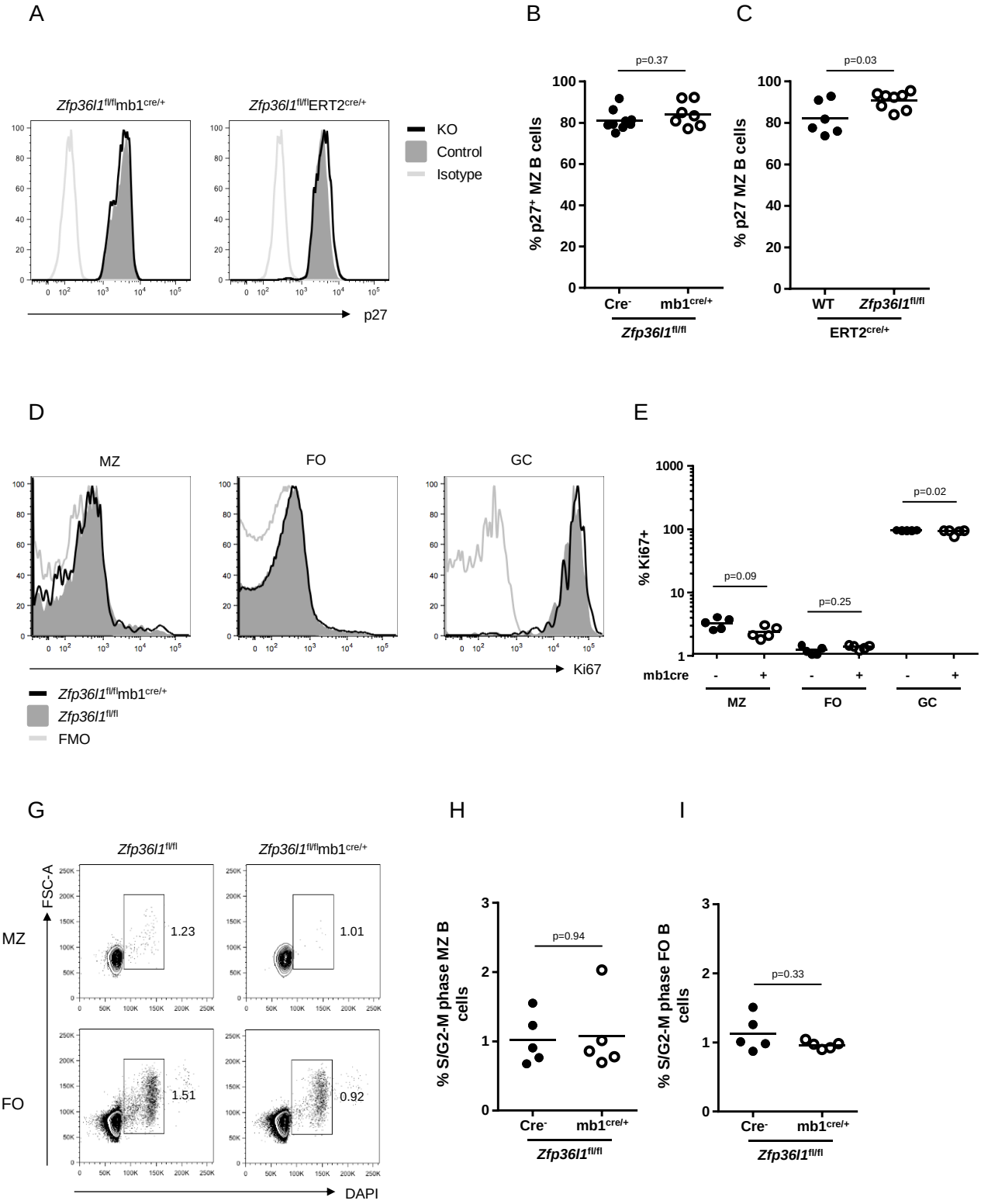
A
Zfp36l1fl/flmb1cre/+
Zfp36l1fl/flERT2cre/+
KO
Control
Isotype
p27
B
p=0.37
% p27+ MZ B cells
Cre-
mb1cre/+
Zfp36l1fl/fl
C
p=0.03
% p27 MZ B cells
WT
Zfp36l1fl/fl
ERT2cre/+
D
MZ
FO
GC
Ki67
Zfp36l1fl/flmb1cre/+
Zfp36l1fl/fl
FMO
E
% Ki67+
p=0.09
p=0.25
p=0.02
mb1cre
MZ
FO
GC
G
Zfp36l1fl/fl
Zfp36l1fl/flmb1cre/+
FSC-A
MZ
FO
1.23
1.01
1.51
0.92
DAPI
H
% S/G2-M phase MZ B cells
p=0.94
Cre-
mb1cre/+
Zfp36l1fl/fl
I
% S/G2-M phase FO B cells
p=0.33
Cre-
mb1cre/+
Zfp36l1fl/fl

A

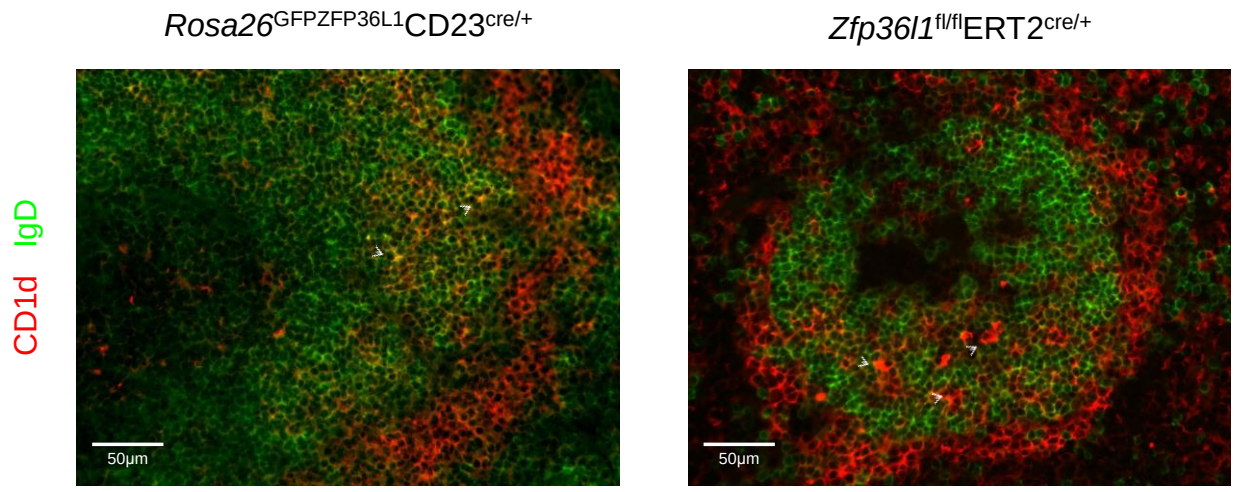
Rosa26GFPZFP36L1CD23cre/+
Zfp36l1fl/flERT2cre/+
CD1d IgD
50μm
50μm

B

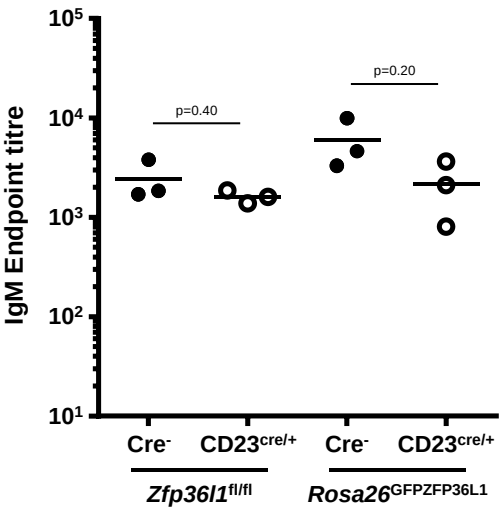
IgM Endpoint titre
10^5
10^4
10^3
10^2
10^1
p=0.40
p=0.20
Cre-
CD23cre/+
Cre-
CD23cre/+
Zfp36l1fl/fl
Rosa26GFPZFP36L1

C

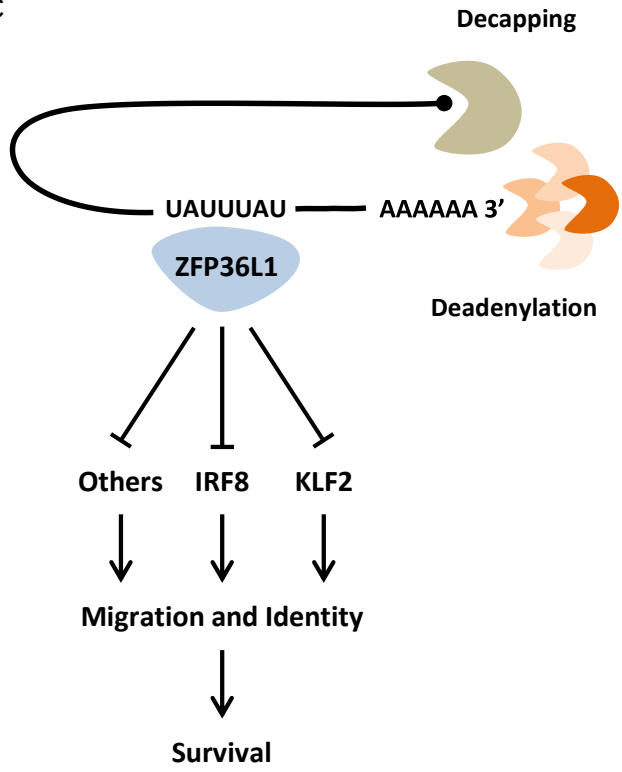
Decapping
UAUUUAU
AAAAAA 3'
ZFP36L1
Deadenylation
Others
IRF8
KLF2
Migration and Identity
Survival

A

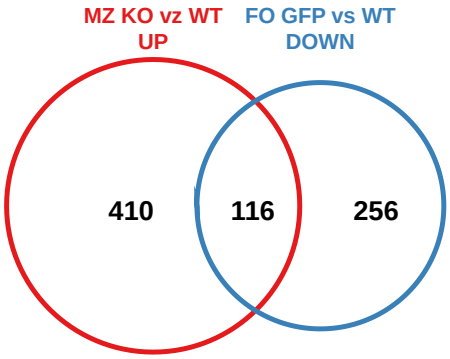
MZ KO vz WT
UP
FO GFP vs WT
DOWN
410
116
256

B

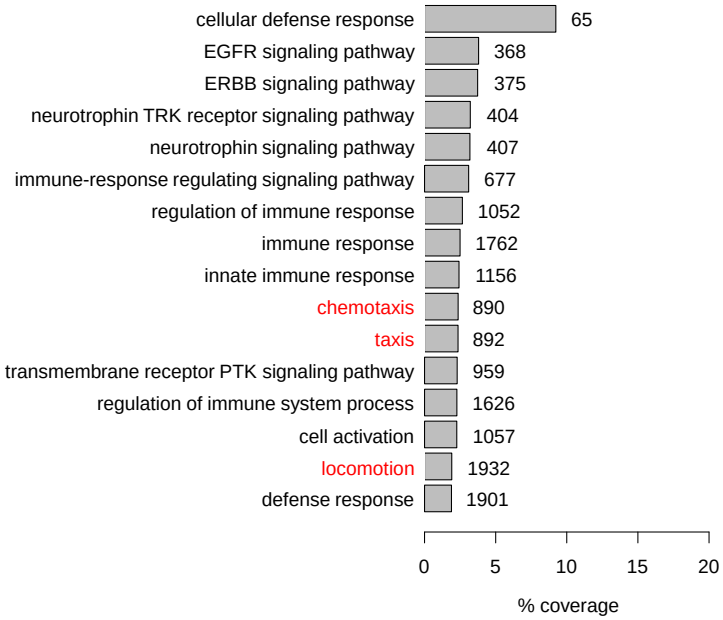
cellular defense response 65
EGFR signaling pathway 368
ERBB signaling pathway 375
neurotrophin TRK receptor signaling pathway 404
neurotrophin signaling pathway 407
immune-response regulating signaling pathway 677
regulation of immune response 1052
immune response 1762
innate immune response 1156
chemotaxis 890
taxis 892
transmembrane receptor PTK signaling pathway 959
regulation of immune system process 1626
cell activation 1057
locomotion 1932
defense response 1901
0 5 10 15 20
% coverage

C

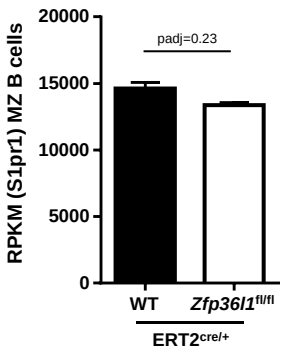
RPKM (S1pr1) MZ B cells
20000
15000
10000
5000
0
padj=0.23
WT
Zfp36l1fl/fl
ERT2cre/+

D

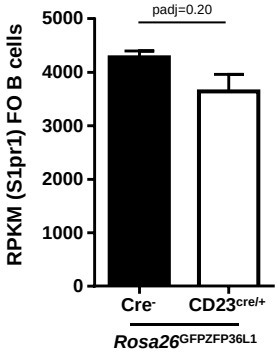
RPKM (S1pr1) FO B cells
5000
4000
3000
2000
1000
0
padj=0.20
Cre-
CD23cre/+
Rosa26GFPZFP36L1

E